Nanomaterial Synthesis in Deep Eutectic Solvents

Sigit Sugiarto [a], Udyani Aloka Weerasinghe [b, c], Joseph Kinyanjui Muiruri [a], Amanda Yu Qing Chai [d], Jayven Chee Chuan Yeo [b], Guan Wang [a], Qiang Zhu [b, c], Xian Jun Loh [b], Zibiao Li [a, b], Dan Kai [a, b, c*]*

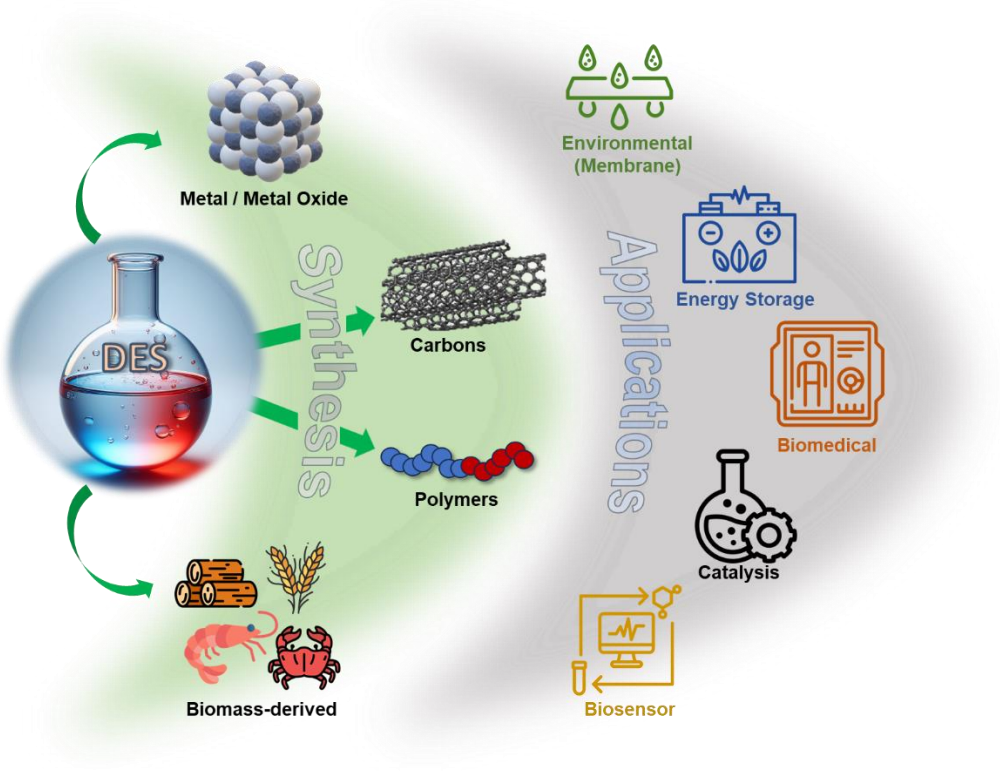
*a. Institute of Sustainability for Chemicals, Energy and Environment (ISCE^2), Agency for Science, Technology and Research (A*STAR), 2 Fusionopolis Way, Innovis, #08-03 Singapore 138634, Republic of Singapore*

*b. Institute of Materials Research and Engineering (IMRE), Agency for Science, Technology and Research (A*STAR), 2 Fusionopolis Way, Innovis #08-03, Singapore 138634, Republic of Singapore*

c. School of Chemistry, Chemical Engineering and Biotechnology, Nanyang Technological University, 21 Nanyang Link, Singapore 637371, Republic of Singapore

d. College of Humanities and Sciences, National University of Singapore, 21 Lower Kent Ridge Rd, Singapore 11907, Republic of Singapore

**Corresponding author: lizb@isce2.a-star.edu.sg; kaid@imre.a-star.edu.sg*



The demand for sustainable nanomaterials drives exploration into eco-friendly solvents like deep eutectic solvents (DESs). Traditionally utilized as extractants, DESs hold potential beyond extraction due to their unique properties. This review discusses DESs' role in crafting functional nanomaterials, covering synthesis processes and potential applications across disciplines, while addressing challenges in sustainable nanotechnology.

Abstract

Nanomaterials have been widely utilized in diverse fields of industry and research. The recent growing demand on sustainable nanomaterials has catalyzed a shift towards eco-friendly and green solvents in materials synthesis. Deep eutectic solvents (DESs) are a new class of green solvents, formed by the combination of two or three components, typically a hydrogen bond donor (HBD) and a hydrogen bond acceptor (HBA), which interact to create a eutectic mixture with a melting point lower than that of the individual components. They have been demonstrated as effective extractants in various fields. However, DESs and their unique properties hold great potential to be utilized beyond extraction. In this review, we would discuss and explore the promising role of DESs in crafting functional nanomaterials. The review starts with the basic chemistry and properties of DES. Additionally, we elucidate the synthesis processes of diverse nanomaterials in DES, encompassing metal/metal oxide, carbons, polymers, and biomasses. We conclude by providing a comprehensive overview of DESs' contemporary role in functional nanomaterials, providing a panoramic view of their potential applications across disciplines. Furthermore, we discuss the opportunities DESs bring to sustainable nanotechnology while addressing the challenges that necessitate innovative solutions.

Keywords: Green solvents, Sustainability, Nanometal, Biomass, Carbon materials

Introduction

Nanomaterials are renowned for their exceptional physicochemical properties due to their high surface area, porosity, and versatility [1], and have become integral in various scientific fields. They exhibit remarkable effectiveness in catalysis, optics, thermodynamics, mechanics, and electronics, making them applicable in many industries and sectors [1], such as metal, ceramics (metal oxide), carbon, polymer, and more. Despite their numerous advantages, conventional nanomaterial synthesis methods are costly, require skilled operators, and lack fundamental mechanism and modeling factors, leading to unstable, toxic, or bioaccumulative nanomaterials, rendering them environmentally unsustainable [2]·[3].

In recent years, deep eutectic solvents (DESs) have garnered significant attention as a series of environmentally friendly and biologically sourced solvents that offer promising applications in nanomaterial synthesis. Initially reported by Abbott and coworkers in 2003 [4], DESs are created through the mixing of hydrogen bond donors (HBDs) and acceptors (HBAs) in varying proportions, resulting in eutectic mixtures that exhibit significantly suppressed melting points when compared to those of the individual components [5]. Due to the growing concerns over the unsustainable organic solvents in materials processing and an increasing demand for green alternatives, DESs have emerged as a promising solution. DESs are distinguished by their affordability, biodegradability, low vapor pressure, non-toxic nature, high viscosity, and ease of synthesis [6]. The tunability of DESs allows for precise adjustment of their thermodynamic properties, including its polarity and conductivity, to meet specific requirements [7]. More importantly, the ability to finely adjust the ratio of HBDs and HBAs in DESs provides a remarkable advantage, as it allows for precise control over their properties, making them highly suitable as specific solvents in nanomaterial synthesis [8], and represent a promising avenue for sustainable nanomaterial production.

The incorporation of DESs in the production of nanomaterials builds upon the fundamental principles of traditional synthesis methods that are commonly employed in aqueous systems. Processes such as electrodeposition, solvothermal methods, calcination, and Pickering-emulsion polymerization [9-14], can be adapted to DES systems, offering distinct advantages over conventional approaches. In the field of nanomaterials, DESs have found significant application in extraction and separation processes [15] DES's low toxicity and natural degradability makes them popular choices for various synthetic strategies, enabling the synthesis of nanomaterials across diverse fields. The continuous development of new eutectic systems further expands the possibilities for innovative nanomaterial synthesis techniques. Recent trends in the past 10 years indicate a rising interest in the use of DESs for nanomaterial production across diverse fields as represented in Figure 1a and 1b.

In addition, Figure 1c shows the timeline of DES-based material innovations, starting from the discovery of DES in 2004, highlighting the significant advancements made in materials science using DES. This growing trend underscores the substantial potential of DESs as a promising pathway for creating innovative and sustainable nanomaterials.

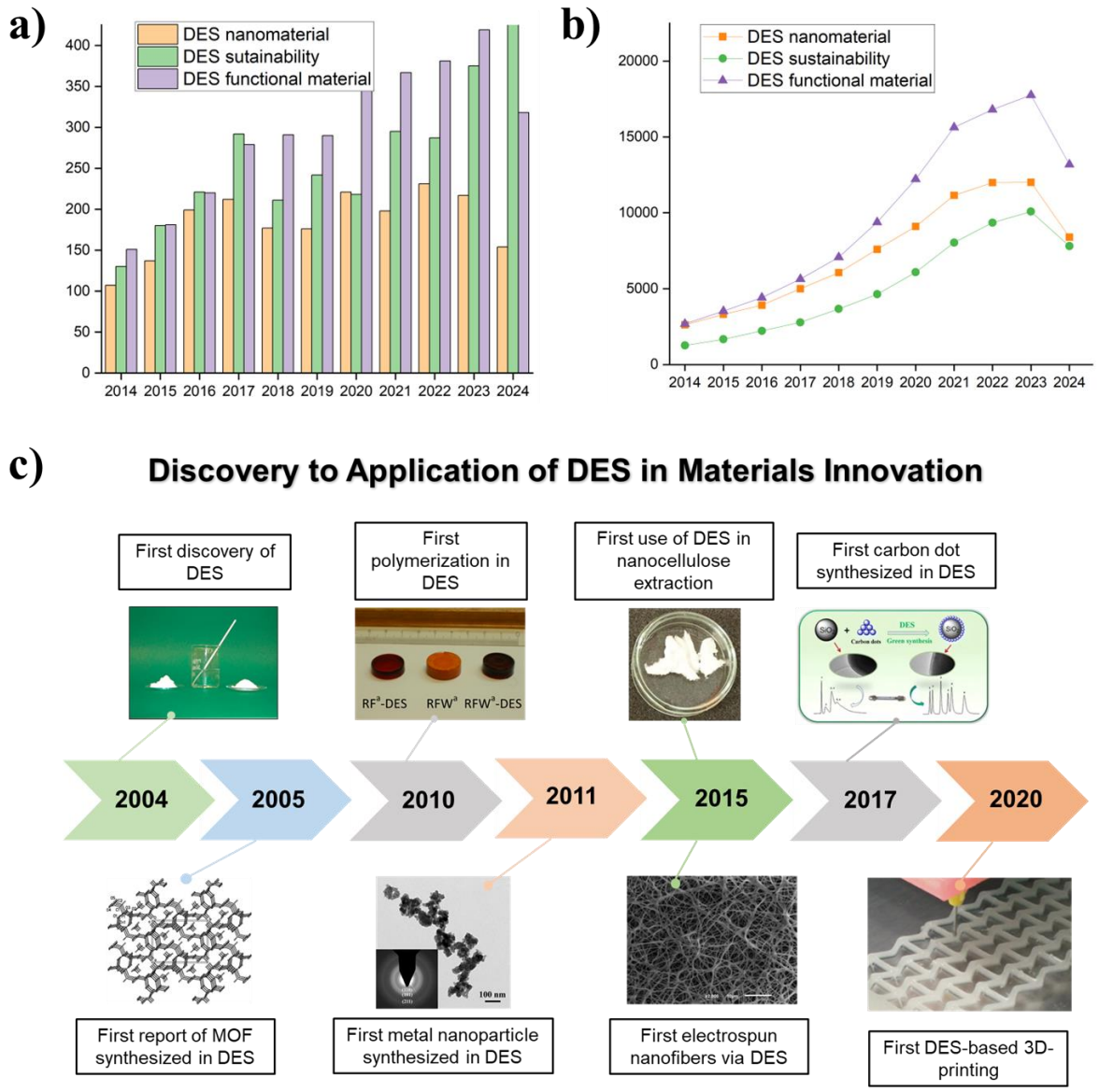


Fig 1. Total count of publication over the past decade, categorized by: **a)** by the number of publications; **b)** by annual citation frequency. With the search terms: "DES nanomaterial", "DES sustainability" and "DES functional material", respectively. According to Web of Science, searched on 11 September 2024; **c)** Timeline of the discovery to application of DES in materials innovation. Images reproduced with permission from references: [4] Copyright (2004), American Chemical Society; [16] Copyright (2005), Elsevier; [17] Copyright (2010), American Chemical Society; [18] Copyright (2011), World Scientific; [19] Copyright (2015), Royal Society of Chemistry.

[20] Copyright (2015), American Chemical Society; [21] Copyright (2017), Springer Science; [22] Copyright (2020), American Chemical Society.

Herein, this review aims to provide a comprehensive overview of utilizing DESs in the synthesis of functional nanomaterials. The composition, types, unique properties, and tunability of DESs, along with their similarities and differences with ionic liquids (ILs) are discussed. We also summarized the synthesis methodologies of different nanomaterials *via* DES systems, including metal and metal oxides, carbons, polymers, and biomass-derived nanomaterials. Furthermore, the review offers insights into the potential applications in various fields as well as sustainability assessments of DES-based synthesized nanomaterials.

2. Fundamentals and Properties of Deep Eutectic Solvents

The term "eutectic" originates from the Ancient Greek word "eútēktos," meaning easily melted [23]. DESs typically consist of two or three pure components capable of forming hydrogen bonds to form a eutectic mixture with a melting point lower than that of each component [24]. The components usually include a hydrogen bond acceptor (HBA) and a hydrogen bond donor (HBD) [25]. Several commonly employed HBAs and HBDs are summarized in Figure 2a, as discussed in the literature [25]. In a typical DES system, Figure 2b illustrates a solid-liquid phase diagram depicting the melting temperature as a function of the mixture composition [26]. In the context of a binary eutectic mixture of compounds A and B, the deep eutectic point signifies the specific composition and the minimum melting temperature at which the melting curves of both compounds intersect [5].

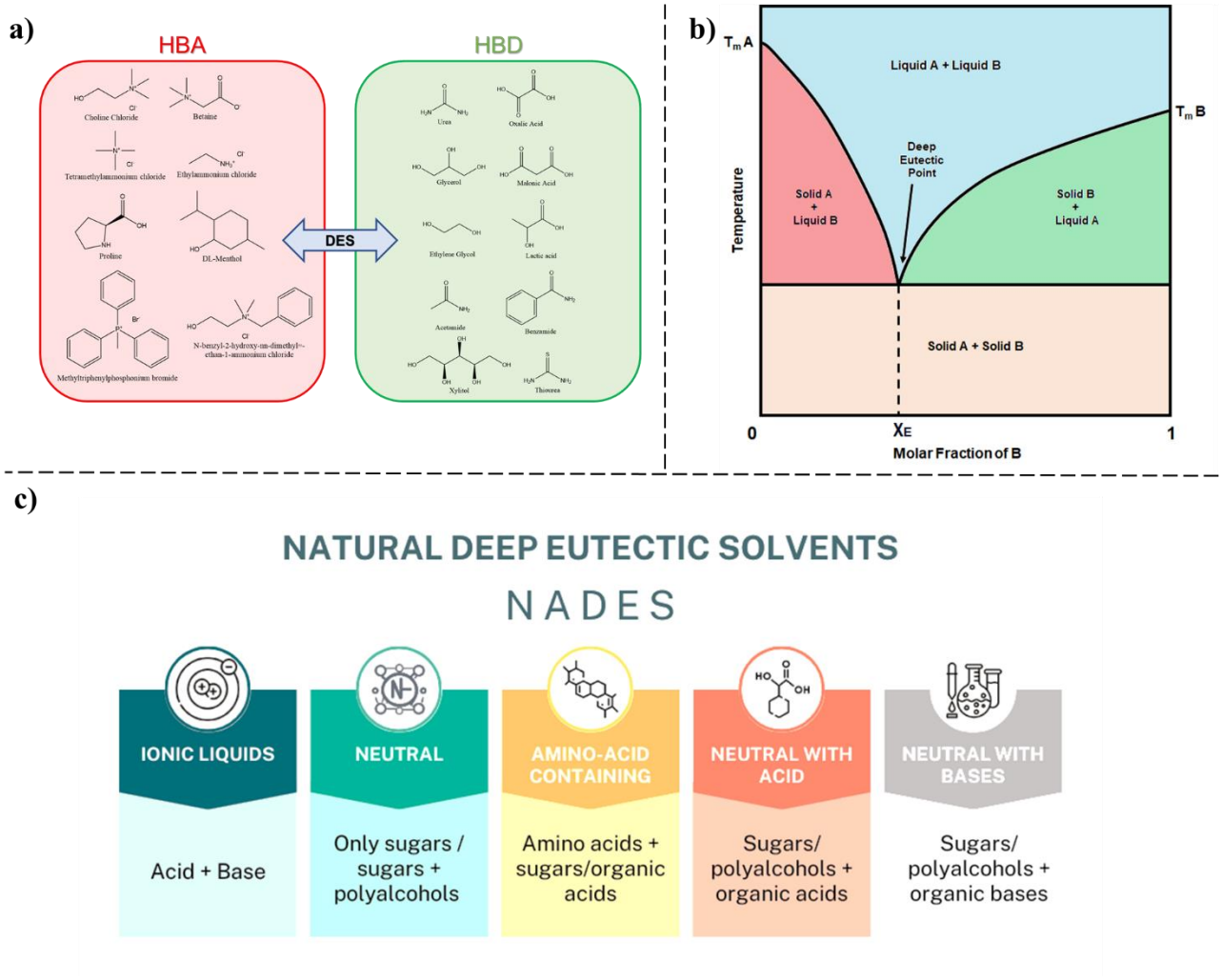


Fig 2. a) Commonly used HBD and HBA for the synthesis of DES. **b)** General solid-liquid phase diagram of a binary eutectic mixture; **c**) Five main categories of NADES.

2.1. Classification of DES

To distinguish between various eutectic combinations, DESs have been categorized into five types (Type I, II, III, IV and V) using the general formula Cat^+X^-zY (Table 1) [27]. The cation Cat^+ is typically represented by an ammonium, phosphonium, or sulfonium group, while the anion X^- represents a Lewis base, commonly a halide [28]. The variable Y represents either a Lewis or Brønsted acid, and the value of z indicates the number of Y molecules that interact with the respective anion [5]. Type V DESs, as recently proposed by Abranches *et al.* [29], are still under discussion and not as widely accepted as other types. We included this classification to reflect the latest advancements and provide a comprehensive view of DES research.

Table 1: Classification of DESs into five different types Reproduced with permission from Ref. [27] Copyright (2021), Elsevier.

Type	General Formula	Terms	Description
Type I	$Cat^+X^-zMCl_x$	M = Zn, Sn, Fe, Al, Ga, In	A quaternary ammonium salt + A metal chloride [30]
Type II	$Cat^+X^-zMCl_x•yH_2O$	M = Cr, Co, Cu, Ni, Fe	A quaternary ammonium salt + A metal chloride hydrate [31]
Type III	Cat^+X^-zRZ	Z = $CONH_2$, COOH, OH	A quaternary ammonium salt + HBD [32] [33] [34] [5]
Type IV	$MCl_x + RZ = MCl_{x-1}^+•RZ + MCl_{x+1}^-$	M = Al, Zn Z = $CONH_2$, OH	Metal chloride hydrate + HBD [35]
Type V	RZ	Z = thymol + menthol	Non-ionic molecular HBA and HBD only [29]

DESs can be classified into five types based on their components as reflected in Table 1. Besides the five common types of DESs, there exist two other novel and non-traditional classes of DESs - therapeutic deep eutectic solvents (THEDES) and natural deep eutectic solvents (NADES) [5]. When one of the components in the DES is an active pharmaceutical ingredient (e.g., ibuprofen, acetylsalicylic acid, DL-menthol etc.), it is classified as a therapeutic deep eutectic solvent [36]. Various literature has shown that when an active pharmaceutical ingredient is delivered to a biological system as a eutectic, it results in substantial improvements in membrane transport effectiveness, intestinal uptake, solubility, and regulated release [37]. Therefore, THEDESs have predominantly been designed for pharmaceutical applications, owing to their capability to enhance the physicochemical characteristics of drugs [38].

Conversely, NADESs are typically formed by the combination of two or more natural compounds, such as organic acids and sugars or amino acids and sugars [39]. The new class of DES emerged when Choi *et al.* discovered NADES [40], an alternative medium to water and lipids for biosynthesis, transport, and storage of compounds with intermediate polarity in living cells. It was observed that several plant primary metabolites, including choline, sugars, and amino acids, can form liquid mixtures resembling DESs when combined in specific compositions [41]. Based on their components, NADESs can be further categorized into five main groups (Figure 2c) [42]. Owing to their biodegradability and biocompatibility, NADES has been rapidly gaining attention for their potential applications in various fields such as pharmaceuticals, cosmetics, and food [43].

In addition to hydrogen bonding, several other noncovalent interactions have been explored in DES systems. For instance, Shi *et al.* discussed a new class of DESs driven by halogen bonding (XB) was developed using quaternary ammonium salts and dihalogens [44]. Another study by Yu and team proposed the concept of "inverted" DESs, where host-guest interactions dominate and primarily involve cations [45]. This innovative approach expands the design possibilities for DESs, particularly for applications in nonaqueous electrolytes. Additionally, the same group also introduced the concept of eutectic molecular liquids (EMLs), which can be formed based on a variety of noncovalent interactions such as π-π stacking, σ-hole, π-hole, κ-hole, and μ-hole bonding, further broadens the understanding of intermolecular forces in liquid systems [46]. The above examples highlight DES systems beyond hydrogen bonding and provide an avenue for diverse interaction mechanisms for specific applications.

2.2. Properties of DES

2.2.1. Physical Properties of DES

All DESs can be distinguished by their characteristic low melting point [47]. For instance, the DES formed using choline chloride (melting point = 302°C) and urea (melting point = 133°C) in a 1:2 molar ratio has a melting point of 12°C, demonstrating a much lower melting point of the DES compared to its pure components [48]. The melting point depression observed in DESs is due to the strong interaction between the HBA and HBD [33]. The melting point of DESs is significantly influenced by the molar ratio of its components, the length of the alkyl chain, the HBA, and the HBD [49].

Density is a fundamental characteristic of liquids that plays a crucial role in defining their physical properties [50]. The majority of DESs, generally having densities in the range of 1.0 to 1.35 $g \cdot cm^{-3}$ at 25 °C, are denser than water. Yet, DESs that include metal salts like $ZnCl_2$ have densities slightly above this range, typically falling between 1.3 and 1.6 $g \cdot cm^{-3}$ [51]. The density of deep eutectic solvents changes with temperature, following a linear decrease as the temperature rises [52]. In accordance with the Hole theory, thermal energy causes variations in local densities, leading to an expansion of free space within the liquid DES system [53]. The density of DESs is determined by the molecular organization and packing, with the existence of voids and vacancies within the liquid DESs also contributing to their variation [49]. Furthermore, the HBD and molar ratio of the DES components can influence the density as well [54].

Viscosity is a significant property of DES, it has been the subject of extensive research and study [55]. The extensive hydrogen bond network between the components of DES is responsible for their typical high viscosity

at room temperature [49]. Some of the most substantial viscosities are found in DESs that involve sugars or amino acids, which ranges from 1000 to 110,000 mPa·s, depending on the sugar used [56]. For instance, a DES composed of sorbitol and choline chloride in a molar ratio of 1:12 exhibits a viscosity of 19,470 mPa·s at 25 °C [57]. Nevertheless, the majority of DESs tend to have relatively elevated viscosities at room temperature, typically exceeding 100 mPa·s[51]. Recently, a data-driven machine learning model was developed to accurately predict viscosity across a wide range of DESs, allowing for more efficient screening and design of novel DESs, particularly in relation to their water content and temperature dependence [58]. While rare, DES exhibiting low viscosity at room temperature exists with the example of hydrophobic deep eutectic solvents based on DL-menthol [59]. The chemical properties of the HBAs and HBDs, along with temperature, water content, molar mass, and molar ratio, all play significant roles in determining the viscosities of DESs leading to the wide range of viscosity values exhibited [60].

The surface tension of DESs serves as an intriguing physical property, providing insights into how the molecular structure affects the interactions between the HBA and HBD in DES mixtures [61]. The higher the intensity of intermolecular forces between the HBA and HBD, the higher the surface tension of DESs [62]. Hence, it is observed that liquids with high viscosity exhibit high surface tensions [63]. In general, surface tension values for DESs ranges from approximately 23.9 $mN \cdot m^{-1}$ to 75.2 $mN \cdot m^{-1}$ [51]. Other than intermolecular forces, the main factors affecting surface tension are the constituents and the composition of the DES mixtures [64]. It has been observed that the introduction of either an additional hydroxyl group or a longer alkyl chain in the quaternary ammonium salt contributes to higher surface tensions [54]. Additionally, surface tension has an inverse relationship with temperature [59].

In addition, other factors including thermal and electrochemical stability, and ionicity also crucial in determining the physical properties of DESs. Thermal stability is a crucial consideration, with DESs generally decomposing through the weakening of hydrogen bonds between HBDs and HBAs at elevated temperatures, unlike ionic liquids (ILs). The choice of HBDs significantly affects the onset decomposition temperature (T_{onset}), as more stable HBDs lead to higher T_{onset} values [65]. Electrochemical stability, particularly the potential windows of DESs, also varies depending on structural factors, such as the type of HBDs and HBAs, influencing their performance in electrochemical applications [66]. Furthermore, ionicity plays a key role in the behavior of DESs. DESs are often referred to as "quasi-ionic liquids" due to their structural similarities with ILs, yet they exhibit lower ionicity due to the lack of free charged species and high viscosity. Despite this, the ionicity of DESs can be tailored by careful selection of components, making them adaptable for specific applications, such as in Li-ion batteries [67].

2.2.2. Chemical Properties of DES

Due to the inverse relationship between viscosity and ionic conductivity, DES tend to have poor ionic conductivity at room temperatures [68]. Consequently, as the temperature rises, the viscosity of the DES decreases while its conductivity increases [69]. This phenomenon occurs due to the disruption of the hydrogen bond network, leading to enhanced ionic mobility within the DES [49]. Besides temperature, ionic conductivity is also affected by the alkyl chain length of the cation, the molar ratio and the chemical properties of DES components [70].

The significance of polarity lies in its representation of a solvent's overall solvation capacity [60]. The polarity of DESs has been evaluated using spectroscopic techniques, specifically by observing the absorbance and fluorescence response of solvatochromic probes [71]. Among the commonly used probes, Reichardt's dye (betaine dye 30) is frequently employed for this purpose [72]. The majority of DESs studied in literature exhibit polarity [49]. By varying the molar ratio of the HBA and HBD, DESs can be tailored to have a wide range of polarity and tunability of their physicochemical properties [73]. Apart from the studies on the polarity, the acidity and basicity of the selected DES system imparts important information regarding the solvation behavior of the system. The Kamlet–Taft solvatochromic parameters can be considered as a useful tool in this regard to further predict the chemical properties of a DES system. This consist of main three parameters namely: α, β and π^* representing the acidity (hydrogen bond donating ability), basicity (hydrogen bond accepting ability) and polarizability of the DES respectively [74]. The comparison and optimization of these parameters, in relation to non-covalent interactions, can yield valuable insights for the effective synthesis of nanomaterials, and the reusability of the DES system [75].

The toxicity of DESs is a critical property to evaluate for various real-world applications [76]. Although DESs have been widely recognized as promising green solvents, there still exists potential toxicity concerns which were first brought up by Hayyan *et al.* [77]. The prevailing assumption is that DESs are non-toxic, primarily due to the natural, biodegradable, and low-toxic properties of their individual starting compounds [78]. Nevertheless, this assumption does not always hold as the toxicity of DESs can vary depending on the specific components used to formulate the mixture [79]. To illustrate, Li *et al.* recently discovered that some amino-acid-containing DESs can be highly toxic contrary to previous beliefs [80]. Comprehensive studies are thus important in evaluating the toxicity of different DES combinations to better understand their effect on living beings and the environment [81].

Like toxicity, biodegradability is another key factor that contributes to DES's eco-friendly profile [82]. The crucial determinant of DESs' biodegradability lies in the neutral nature of their hydrogen bond donors and acceptors,

resulting in a natural mixture that can be easily metabolized by bacteria and fungi [49]. A common method to test for biodegradability is the closed bottle test, in which a bottle containing the substance of interest and microorganisms is kept in a controlled environment, and the microbial activity is monitored over a specified period [83]. Although previous studies have shown that DESs are readily biodegradable, it is still too early to generalize due to the limited number of studies done and the wide variety of DES combinations that have yet to be studied [84].

3. Nanomaterial fabrication via DES

The application of DES has revolutionized the landscape of nanomaterial production, offering a dynamic and versatile platform for engineering innovative materials. The synergy between green chemistry principles and nanotechnology, DES-driven production methods hold tremendous potential for developing nanomaterials with enhanced functionalities. Unlike conventional solvents, DESs offer a greener alternative that reduces environmental impact while enhancing synthesis efficiency and selectivity. Their low volatility, non-flammability, and broad solubility provide precise control over the synthesis process. This section delves into the transformative role of DES in nanomaterial synthesis, highlighting its unique properties that facilitate precise control over the morphology, size, and surface characteristics of nanomaterials.

3.1. Metal/Metal oxide-based Nanomaterials

DES are deployed as sustainable solvents to fabricate metal and metal oxide nanomaterials. In contrast to conventional solvents, DES may serve multiple functions as reducing agents and stabilizer as confirmed by the recent work from Torrente-Murciano's group, elucidating the role of the reline based DES in the synthesis of gold nanoparticles [85]. In another earlier study, Baker *et al.* reported that gold nanocrystals could be made from DES in a in scalable and sustainable way using flow processes [86]. Sun *et al.,* reported the synthesis of gold nanoparticles in DES with shape-controlled for the first time. The study demonstrated that the shape control was simply realized by varying the ratio of a small amount of water in the DES [87]. The SEM image of star-shaped Au nanoparticles prepared from the study is shown in Figure 3a. An electrochemical method has also been developed to prepare nanoporous gold electrodes by alloying and dealloying Au–Zn alloy in DES comprised of $ZnCl_2$–urea [88]. The work highlights the importance of metal-based DES for synthesis of nanoporous metal electrodes.

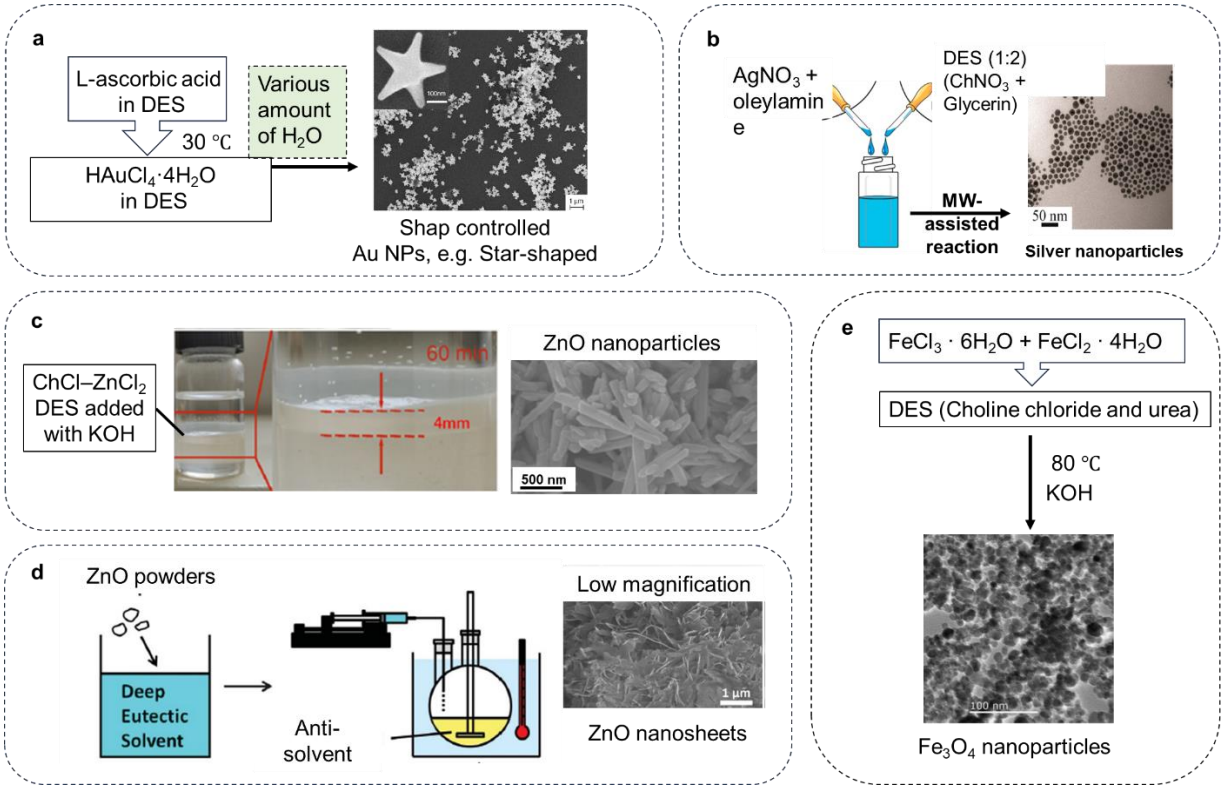


Fig 3. Schematic synthesis of representative **a)** controlled shaped Au NPs; **b)** AgNPs; **c)** ZnO nanoparticle; **d)** ZnO nanosheets; **e)** Fe_3O_4-DES nanoparticles, prepared from DES. (Image in **a** reproduced with permission from Ref. [87] Copyright (2018), Wiley; Image in **b** reproduced with permission from Ref. [89] Copyright (2018), American Chemical Society; Image in **c** reproduced with permission from Ref. [90] Copyright (2013), Elsevier; Image in **d** reproduced with permission from Ref. [91] Copyright (2023), Royal Society of Chemistry; Image in **e** reproduced with permission from Ref. [92] Copyright (2012), Royal Society of Chemistry.

Nanoparticles of silver have also been synthesized utilizing DES. Using DES-based green tea extract, silver nanoparticles were prepared in an ecofriendly biogenic manner [93]. Baker's group further made silver nanoparticles in DES with the assistance of microwave reaction [89], and in a scalable, flow process. Silver nanoparticles were also prepared from malonic acid based ternary DES [94].

Cerium nanoparticles have also been synthesized from ethaline DES, deploying cerium chloride as precursor, and using hydrazine sulfate as the reducing agent [95]. Ceria (cerium oxide) nanoparticles represent one of the popular types of metal oxide nanoparticles that have also been prepared using DES. Torrente-Murciano's group reported the synthesis of nanostructured ceria using reline-based DES, which allows morphology and porosity control. The method utilizing DES represents one of the less energy-intensive routes [96]. Iqbal *et al.* further reported that use of DES solvent resulted high yield and stability of ceria nanoparticles as compared to acetic acid [97].

Fe_3O_4 nanoparticles have been widely explored in magnetic separation and have also been made in DES. Chen *et al.* reported the synthesis of spherical Fe_3O_4 magnetic nanoparticles by co-precipitation in DES (choline chloride/urea) [90]. The magnetic Fe_3O_4 nanoparticles made in DES show higher absorption capacity then those made from deionized water. Hammond *et al.* further reported the structural evolution of iron forming iron oxide in a DES-solvothermal reaction, and the group reported evidence for a choline enriched boundary layer at the nanoparticle interface using SANS/SAXS analysis [98]. Another type of magnetic nanoparticles, i.e. mesoporous alpha-manganese dioxide (α-MnO_2) have also been synthesized from manganese(II)-based DES comprised of $MnCl_2$•$4H_2O$ and acetamide (1:7 molar ratio), where the DES acts as solvent and reducing reagent [99].

Using metal-based DES, Chen *et al.* reported the synthesis of ZnO, CuO, Fe_2O_3 and Co_3O_4 nanoparticles [91]. Metal-based DES were made by mixing metal salts with ChCl, and nanoparticles were prepared by adding KOH solution into the ChCl–MCl_x DESs. In another report, mesoporous ZnO nanosheets with single crystalline were prepared with a green antisolvent method [92]. Besides single metallic oxide, mixed metal oxide such as spinel CoFe oxide porous nanosheets ($Co_{2.698}Fe_{0.302}O_4$ nanosheets) has also been prepared [100]. In addition to its role as a solvent, DES may also be used as a functional agent, for example, carbon nanotubes (CNT)/$ZnCo_2O_4$ nanostructure have also been prepared using DES as both a solvent and functional agent [101].

MXenes are two-dimensional materials, typically consist of transition metal carbides, nitrides, or carbonitrides, with excellent conductivity and versatile applications, such as energy storage and water purification. However, exfoliating MXenes can be challenging due to oxidation when using aqueous solutions. Traditional solvents are often toxic or expensive, making them unsuitable for large-scale use. DES offer a green, low-cost, and effective alternative, providing antioxidative properties that prevent oxidation and improve the exfoliation process. Shan *et al.* presented a novel method for preparing Ti_3C_2 MXene using a DES-assisted electrochemical ultrasonic exfoliation [102]. Using a low-cost DES (choline chloride–urea) and water mixture as the electrolyte, the DES played roles in intercalation, interlayer expansion, and anti-oxidation. This method produced MXene with fewer layers, larger interlayer spacing, higher hydroxylation, and greater oxidation resistance, resulting is MXene–DES which demonstrated excellent mechanical properties, a wide voltage window, and high specific capacitance. Similarly, Gong *et al.* developed a novel water-free etching method to synthesize few-layered $Ti_3C_2T_x$ MXenes using DES at near-ambient temperatures [103]. This method avoids water and leverages the macromolecular structure of the solvents, which resulted in MXenes with abundant -O terminations and low oxidation. The resulting MXenes showed excellent specific capacitance and impressive long-term stability, retaining 97%

286 capacitance over 50,000 cycles. Table 2 summarizes the different types and roles of DES in metal and metal oxide-
287 based nanomaterials.

Table 2. Summary table of the types and functions of DES in metal and metal oxide-based nanomaterials.

Type of DES	Function of DES	Nanomaterial / Application	Ref.
Choline chloride-urea (Reline)	Reducing agent, stabilizing agent	Small gold nanoparticles (<3 nm) with narrow size distributions.	[85]
Choline chloride-urea	Solvent for shape-controlled synthesis of gold nanoparticles (Au NPs)	Star-shaped gold nanoparticles (Au NPs) with unique facets. Water content adjustment in DES yields diverse Au NP shapes, including snowflake-like and nanothorns.	[87]
$ZnCl_2$–urea	Fabrication of nanoporous gold (NPG)	NPG electrodes with large surface area and electrochemical activity. Detection of water pollutants with high sensitivity and low detection limits. Potential electrochemical sensing platform.	[88]
C**holine nitrate-glycerol**	Rapid synthesis of organosoluble AgNPs	Simple, ecofriendly synthesis of AgNPs within a halide-free DES, with potential for anisotropic growth of shape-controlled AgNPs.	[89]
Choline chloride-urea	Synthesis of spherical Fe_3O_4-DES magnetic nanoparticles (ca. 10.5 nm) via co-precipitation of Fe^{3+} and Fe^{2+} ions	Spherical Fe_3O_4 magnetic nanoparticles with improved Cu^{2+} adsorption capacity.	[90]
Metal chloride-Choline chloride	Raw materials and medium for nanomaterial fabrication	Synthesis of ZnO, CuO, Fe_2O_3, and Co_3O_4 nanoparticles with low band gaps for effective pollutant degradation.	[91]
Choline chloride-urea	Green antisolvent process for synthesis	Single-crystalline mesoporous ZnO nanosheets with ultrathin structure, suitable for photocatalytic degradation of pollutants.	[92]
Betaine-Glycerol, G**lycerol-Urea**, **Betaine-Urea**	Green tea extract preparation	Enhanced synthesis of silver nanoparticles (AgNPs) with higher catechin levels and synthesis efficiency compared to water-based GTE. DESs serve as efficient extraction solvents and surface modifiers for AgNPs.	[93]
Malonic acid with glutamine and glucose/fructose ternary	Solvent for synthesizing silver nanoparticles (AgNPs)	Silver nanoparticles with antifungal behavior.	[94]
Choline chloride-ethylene glycol (Ethaline)	Medium for the synthesis of metal nanoparticles (MNPs)	Synthesis of cerium nanoparticles (CeNPs) incorporated into a suspension for sensor modification providing enhanced performance.	[95]
Reline-based	Synthesis of nanostructured ceria with control of morphology and porosity and acts as latent supramolecular catalyst	Nanostructured ceria with enhanced surface area, reactive oxygen vacancies, and oxygen storage capacity.	[96]
CTAB (cetyltrimethylammonium bromide)/acetic acid	Synthesis of stable, crystalline, and mesoporous ceria nanoparticles	Synthesis of ceria nanoparticles with high removal efficiency of flumequine (FLU) under UV-C irradiation.	[97]

Choline chloride–urea	Serves as a solvent and enables structural evolution	Formation of iron oxide nanoparticles through a DES-solvothermal reaction. The analysis reveals the presence of a choline-enriched boundary layer at the nanoparticle interface.	[98]
$MnCl_2$•4H2O-acetamide	Acts as a solvent and reducing agent	Preparation of mesoporous alpha-manganese dioxide (α-MnO_2) nanoparticles by using DES composed of $MnCl_2$•$4H_2O$ and acetamide, where the DES functions both as a solvent and reducing agent.	[99]
Choline chloride -urea	Medium for the synthesis of a precursor material called layered double hydroxide (LDH) analogue structure of CoFe	DES-synthesized LDH precursor transforms into porous CoFe oxide nanosheets with small grain size, high surface area, and magnetic separability, serving as efficient adsorbents for rapid removal of organic waste and toxic heavy metals.	[100]
CTAB-glycerol	Utilized as both a solvent and functional agent	Preparation of carbon nanotubes (CNT)/$ZnCo_2O_4$ nanostructures, showcasing the dual role of DES in the synthesis process.	[101]
Choline chloride-urea	Intercalation, interlayer expansion, anti-oxidation	Preparation of Ti_3C_2 MXene with fewer layers, larger interlayer spacing, higher hydroxylation, and greater oxidation resistance. Used in a flexible solid-state supercapacitor with excellent properties.	[102]
Choline chloride-urea	Water-free etching	Synthesis of few-layered $Ti_3C_2T_x$ MXene with abundant -O terminations and low oxidation. Exhibits high specific capacitance and long-term stability.	[103]

3.2. Carbon-based nanomaterials

3.2.1. 0-dimensional carbon (quantum) dots

Carbon (quantum) dots represent a special class of 0-dimensional carbon nanomaterials and have found many applications, including bioimaging and sensing. DES is a useful solvent for preparation of carbon dots. Nitrogen and chloride-doped carbon dots have been prepared from urea (carbon source) and DES (choline chloride based as solvent) in one-step hydrothermal reactions [104-106] (Figures 4a & 4b). Variation of DES could also have impact on the synthesis of carbon dots. Tabaraki *et al.* reported the comparison of using DES with and without water as the solvent to synthesize carbon dots. They found the carbon dots prepared from water/DES possess higher fluorescent quantum yield [107]. The DES solvent also influences the surface chemical composition and morphology. In another study, Zhao *et al.* reported the use of metallic DES for synthesis of citric acid derived carbon dots doped with Cu and Cl [108]. This work highlighted the use of metallic DES as a solvent and passivation agent. Likewise, capitalizing on DES as a passivation agent, Ren *et al.* documented the hydrothermal synthesis of near-infrared fluorescence carbon quantum dots with polyethylene glycol-based DES, comprising of p-phenylenediamine (PPD) and polyethylene glycol 400 (PEG 400) [109]. Ternary DES has been used as an environmentally friendly way pretreatment for low-cost chamomile residue and synthesis of carbon dots using solvothermal method [110].

3.2.2. 1-dimensional Carbon nanotubes

Unlike carbon dots, where DES finds varied applications, its use in relation to carbon nanotubes (CNTs) predominantly revolves around their functionalization. Alsaadi's group reported a series of work on the functionalization of CNTs using DES, comprising of glycerol or ethylene glycerol as hydrogen bond donor and methyltriphenylphosphonium bromide (MTPB), benzyltriphenyl-phosphoniumchloride (BTPC), allyl triphenyl phosphonium bromide, N,N-diethyl ethanol ammonium chloride and choline chloride salt (ChCl), respectively [111-114]. The same group also further developed a feedforward artificial neural network-based model to predict the using of DES-functionalized CNTs for removal of phenolic compounds in water [115]. The model for prediction of 2,4-dichlorophenol removal was in high competence with an R^2 value of 0.99. The method by Alsaadi's group involves the use of harsh acid treatment combined with refluxing. Furthermore, Ye *et al.* reported the functionalization of multi-walled carbon nanotubes (MWCNTs) using long chain betaine-based deep eutectic solvents (DESs) by mechanical milling [116]. The use of DES for CNTs surface functionalization requires proper dispersion in the medium. Zaib *et al.* studied the specific impacts of three critical factors on the dispersion of single walled carbon nanotubes (SWNTs) in choline chloride-glycerol DES: (i) mass% in water, (ii) sonication

energy input (J/mL), and (iii) concentration of SWNTs [117]. This study contributes to enhancing the understanding of preparing sustainable and economically feasible DES nanomaterial dispersions.

3.2.3. 2-dimensional Graphene (oxide)

Like in the case of CNTs, DES are frequently used as functionalization agent for 2-dimensional graphene (oxide). AlSaadi and colleagues also reported the utilization of DES for functionalizing 2-dimensional graphene, thereby introducing novel functional groups onto the graphene surface [111] (Figure 4c). The DESs formed by the prepared choline chloride and hydrogen bond donors (namely, quaternary salts and alcohols) effectively serve as favorable dispersion media for graphene. In another study, DES-modified graphene and graphene oxide have been prepared on silica support through covalent bonds and used as adsorbents [118]. Magnetic graphene nanoparticles (Fe3O4@GO nanoparticles) were synthesized through DES coating, serving as adsorbents with the advantage of effortless recovery [119]. The two studies highlight the strategies of using DES for modification of hybrids graphene (oxide) materials, i.e., graphene oxide with silica, graphene oxide with iron oxide. In addition to the applications in the field of adsorbents, CO_2-philic separation membrane based on DES modified graphene oxide was constructed by nanoconfining DES into nanoslits, which relies on hydrogen bonds formation between graphene oxide nanosheets with the active sites of DES [120]. Choline chloride-alcohol-based DES has also found application as a porogen for the fabrication of monolithic chips doped with graphene oxide, owing to the effective dispersion of graphene oxide within the DES medium [121] (Figures 4d and 4e).

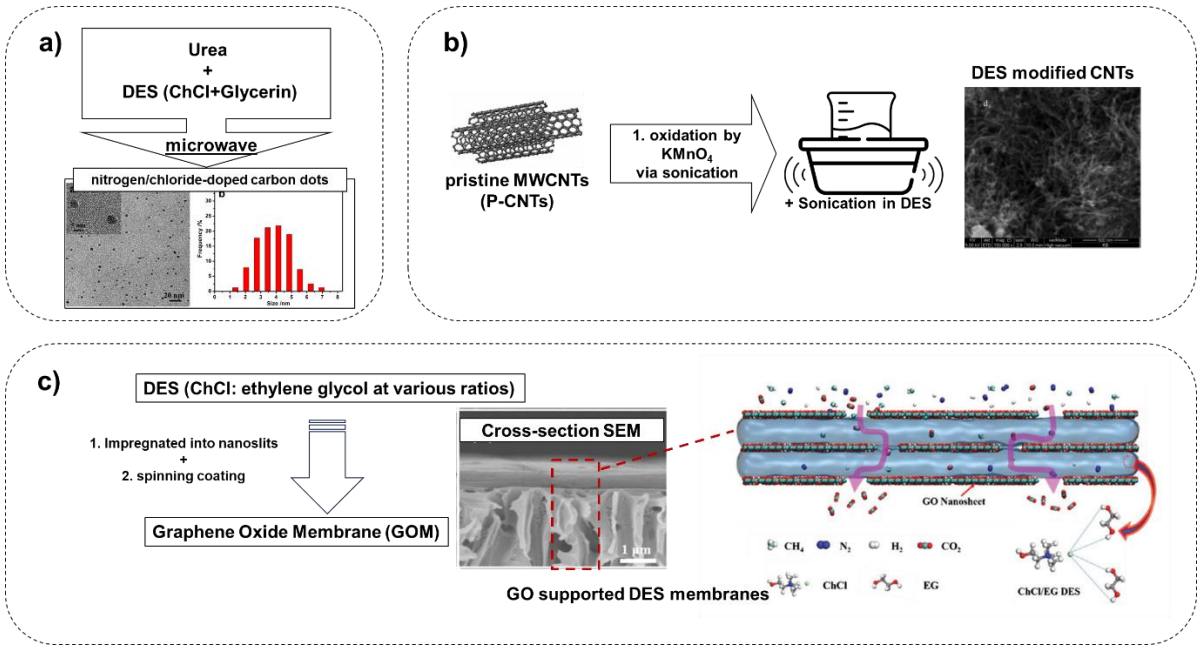


Fig 4. a) Synthetic scheme, HRTEM image and particle size distribution of the nitrogen/chloride-doped carbon dots synthesized from DES; **b)** Synthetic scheme, FESEM image for DES modified multiwalled CNTs; **c)** Synthetic scheme, SEM images for cross sections of GO supported DES membrane, and schematic diagram of the selective solution-diffusion process of gas molecules through the ChCl:EG filled laminated GO nanoslits (Image in **a** are reproduced with permission from Ref. [104] Copyright (2018), American Chemical Society; Images in **b** are reproduced with permission from Ref. [111] Copyright (2016), Elsevier; Images in **c** are reproduced with permission from Ref. [121] Copyright (2020), Elsevier.

However, despite the growing research on the utilization of DES for various nanomaterial syntheses and functionalization, it was noted that comprehensive reports pertaining to the application of DES in the synthesis or functionalization of three-dimensional nanodiamonds and nanohorns are still notably absent from the existing literature. This underscores a potential avenue for further exploration and investigation in the realm of utilizing DES for advanced nanomaterial fabrication in these specific contexts. Overall, the advantages of using DESs over other solvents, including their environmental friendliness, tunability, and ability to facilitate complex reactions under mild conditions, make them a compelling choice for nanomaterial synthesis. Table 3 summarizes the various types and roles of DES in carbon-based nanomaterials.

3.2.4. Advanced Carbon-Based Materials

In recent years, carbon-based materials have garnered significant attention due to their unique properties, such as high electrical conductivity, mechanical strength, and tunable surface chemistry. Among these, doping carbon materials with heteroatoms like nitrogen, sulfur, and oxygen (N, S, O) as well as the development of graphitic carbon nitride (g-C_3N_4)-based materials, have opened new avenues in catalysis and photocatalysis. These materials offer enhanced chemical reactivity, stability, and performance in various applications, from energy storage to environmental remediation.

One notable study reported the development of multi-doped carbon composite materials using a DES system through one-step pyrolysis. The resulting Co_9S_8–Ni_3S_2@NSOC (N, S, O-doped carbon) composite demonstrated excellent catalytic properties, achieving nearly 100% biomass conversion and 98.8% selectivity, along with enhanced durability in electrocatalytic applications. Zhang *et al.* highlighted the role of DESs in the preparation of complex doped carbon structures and provides a foundation for further exploration of carbon-based catalysts in energy conversion and environmental applications.

77 Another promising work by Mou *et al.* integrated amorphous ZrO_2 into g-C_3N_4 via a simple DES-based pyrolysis
78 method. The resulting g-C_3N_4/ZrO_2 composite showed superior performance in solar-driven NH_4^+ evolution,
79 achieving yields significantly higher than its individual components . This enhanced photocatalytic activity is
80 attributed to the efficient separation of electron-hole pairs and the rapid transfer of photogenerated electrons,
81 making g-C_3N_4-based materials a compelling candidate for green energy applications.

82 These studies illustrate the growing potential of DES-facilitated synthesis of advanced carbon-based materials,
83 emphasizing the versatility of DESs in tailoring material properties for high-performance catalytic and
84 photocatalytic systems.

Table 3. Summary table of the types and functions of DES in carbon-based nanomaterials.

DES Type	Function of DES	Nanomaterial Produced / Application	Ref.
Choline chloride–glycerine	Serves as a solvent for controlling the synthesis of carbon dots in the absence of water	Dual-functional nitrogen- and chloride-doped carbon dots (N/Cl-CDs) for intracellular pH sensing, multicolour imaging, and detection of Cytochrome	[104-106]
Choline chloride-urea	Serves as a medium for the synthesis of nitrogen and chloride co-doped carbon dots (N/Cl-CDs), for the one-step hydrothermal synthesis process	Nitrogen and chloride co-doped carbon dots (N/Cl-CDs) for Hg^{2+} detection, photocatalytic antifungal activity and fluorescence labelling and imaging	[104-106]
C**holine chloride/acetamide**	Serves as a solvent for the synthesis of N-doped carbon dots (N-CDs) by microwave irradiation	N-doped carbon dots (N-CDs) as fluorescent probe, and cetirizine detection in biomedical applications	[107]
$CuCl_2.2H_2O$ and ethylene glycol/choline chloride	Used as green solvent and passivation agent, to provide a sustainable and non-toxic medium for the hydrothermal synthesis process, control the surface properties and enhance stability	Green synthesis of Cu, Cl co-doped Carbon Dots (Cl-CDs) with tailored catalytic properties. Used in catalysis and calorimetric sensing	[108]
PEG-based	Used as a precursor for the synthesis of CQDs	Near-infrared fluorescence carbon quantum dots (CQDs) as fluorescence detection	[109]
Ternary DES (choline chloride, lactic acid, and urea)	Used to pretreat chamomile residue to prepare it for subsequent processing and carbon dot (CDs) synthesis	High quantum yield CDs as a fluorescent probe	[110]
Methyltriphenylphosphonium bromide (MTPB) and benzyltriphenylphosphonium chloride (BTPC)/glycerol (Gly)	Used as functionalization agents for carbon nanotubes (CNTs)	Functionalized CNTs adsorbents for removal of As^{3+} from water	[111]
Allyl triphenyl phosphonium bromide (ATPB)/glycerol	Serves as a novel agent for functionalizing carbon nanotubes (CNTs)	Functionalized CNTs adsorbents for removal of Hg^{2+} from water	[111-114]

Choline chloride/ethylene glycol	Used as functionalization agents for multi-walled carbon nanotubes (CNTs)	Novel functionalized CNTs adsorbents for removal of 2,4-dichlorophenol (2,4-DCP) from aqueous solutions	[115]
Long chain betaine	Used for the non-covalent functionalization of multi-walled carbon nanotubes (MWCNTs).	Modified MWCNTs for adsorption of bromophenols from kelp and seaweed	[116]
Choline Chloride-Glycerol	Used as a medium to disperse single-walled carbon nanotubes (SWNTs) into smaller bundles	Dispersion of SWNTs with promising implications across various nano-manufacturing fields	[117]
Choline chloride-based	DES and IL are used to modify graphene (G) and graphene oxide (GO) to enhance their adsorption properties	functionalized GO@silica nanomaterial as adsorbent and Solid-phase extraction (SPE)	[118]
Choline chloride-based	Used to coat magnetic graphene nanoparticles, resulting in Fe3O4@GO-DES	Fe3O4@GO-DES for preconcentrating of methadone	[119]
Choline chloride/ethylene glycol	Used as a CO_2-philic material for the construction of a separation membrane	Highly CO_2-philic separation membrane constructed by nanoconfining ChCl/EG deep eutectic solvent into graphene oxide nanoslits, for selective CO_2 separation	[120]
ChCl and different type of alcohols	Used in conjunction with carboxylated graphene oxide (GO) to create a matrix suitable for the incorporation of GO into a monolithic chip.	Monolithic chip that incorporates carboxylated graphene oxide (pAS–COOH–GO) into its structure for solid-phase extraction (SPE) of polycyclic aromatic hydrocarbons (PAHs)	[121]

3.3. Polymeric Nanomaterials

3.3.1. DES as solvent

DES acts as a solvent medium to dissolve and facilitate the polymerization or synthesis of nanomaterial precursors, exhaustively applied in nanomaterial synthesis after the pioneering work reported in 2012 by Zhang *et al*. [122] DES enables effective dissolution of a wide range of polymers and polymer precursors, enabling uniform mixing and different polymerizations reaction. Adjusting DES's polarity enables fine-tuning reaction conditions and control over the resulting nanomaterial properties. In earlier work, Fernandes *et al*. [123] utilized choline chloride (ChCl) (HBA) and 1,2-ethanediol (HBD) (known as propeline) as a solvent to prepare polyaniline (PANI) using potentiodynamic and potentiostatic electrochemical procedure. The potentiostatic-prepared films presented a homogenous and denser matrix of PANI fibers of about 80 – 100 nm width with 150 – 250 nm pores. Choline chloride (ChCl) (HBA) and urea (HBD) are also other popular choice[124, 125]. For instance, Kumar and Singha [126] reported a DES, made of ChCl/urea, as a solvent for the polymerization-induced self-assembly (PISA) of 2-hydroxyethyl methacrylate (HEMA) and its block copolymerization with methyl methacrylate (MMA) forming self-assemble PHEMA-*b*-PMMA spherical particles of 60 to 70 nm. Likewise, Bednarz and team [127] copolymerized renewable itaconic acid (IA) with N,N'-methylenebisacrylamide (MBA) in DES based on ChCl. The resultant branched copolymers have a hydrodynamic size ranging from 10 to 100 nm and an average monomer composition of 7–9 mol% of MBA. In addition, DES also has dual roles in the new class of functional gel, known as supramolecular eutectogels, serving as both a reaction medium and a non-aqueous sol-gel preparation of silica and electrolyte, finding applications in flexible batteries and supercapacitors. Ruiz-Olles *et al.* [128] discovered a simple, commercially relevant compound, 1,3:2,4-Dibenzylidene-d-sorbitol (DBS), as a gelator to self-assemble due to the intermolecular non-covalent interactions into supramolecular gels in ChCl combined with alcohols/ureas DES solvent. The DBS successfully immobilizes the DES and results in self-assembled gels with nanofibrillar morphologies of 20 – 50 nm, as evidenced in the SEM images. Likewise, Gu *et al.* [129] also utilized a ChCl/alcohol DES to produce complexes of natural guanosine and H_3BO_3 with excellent gelation capacity. The self-assembled supramolecular eutectogels are mediated by cation-templated G-quartets formation and subsequent stacking into G-quadruplex nanowires, highly dense and entangled fibrils with diameters less than 100 nm. The exceptional solvent-induced chiral inversion on the boronate ester formation also contributed to a high ionic conductivity (up to 7.78 mS cm^{-1}), high thermal stability, excellent thixotropic/injectable properties, and electrochromic activity.

3.3.2. Polymerization with DES

The integration of polymerizable DES (PDES) or DES monomers has revolutionized the landscape of polymeric nanomaterial synthesis and served the dual function of both solvent and building blocks for the nanomaterials. DES monomers polymerized into polymers due to the monomer bearing a hydrogen bond-forming molecule with the unreacted DES component as part of the polymeric hybrid structure, first reported by Mota-Morales *et al.* [130] in 2011, using DES based on acrylic acid (AA) or methacrylic acid (MAA) with ChCl. The research group [131] utilized AA (HBD) and ChCl (HBA) as DES to prepare macroporous PAA-CN_xMWCNT composites using frontal polymerization (FP). The DES has outstanding efficiency in solubilizing and dispersing N-doped carbon nanotubes (CNxMWCNT) in the polymerizable DES and can control FP's self-propagating nature. The group reported the optimum molar ratio of 1.6: 1 (AA: ChCl) due to the well-balanced performance in terms of viscosity and density of double bonds required for DES-assisted FP. The resultant PAA-CN_xMWCNT morphology showed that PAA was coated homogeneously with every single CNT of 20 – 50 nm. In another interesting work, PDES composed of AA/ChCl were used as backfilling agents, and in-situ photopolymerized AA with crosslinkers and acrylates in the delignified wood [132]. Similar approaches employing AA as a DES monomer were reported in bacterial cellulose [133] and phytic acid [134].

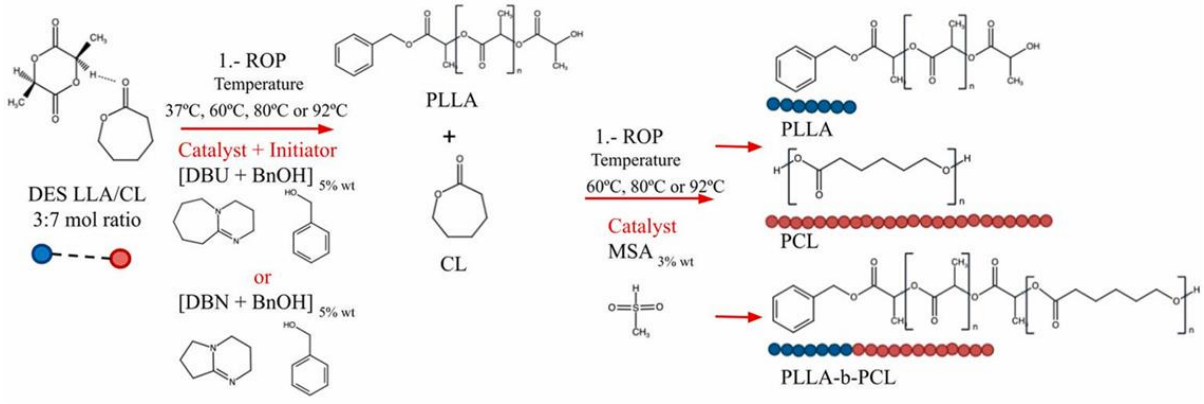


Fig 5. Sequential Ring-Opening Polymerization of the DES composed of LLA/CL (3:7 M ratio) at different temperatures. DBU and DBN organocatalysts were used for the selective ROP of LLA in the first step, and they were added together with the initiator BnOH (1:1, M ratio). MSA was used as a second organocatalyst to start the ROP of CL in the presence of the already-formed PLLA. Reproduced with permission from Ref. [135]. Copyright (2022) Elsevier.

Recently, Mota-Morales and co-workers [135] demonstrated ring-opening polymerization (ROP) of eutectic mixtures of L-lactide and ε-caprolactone using a new catalyst 1,5-Diazabicyclo[4.3.0]non-5-ene (DBN), as shown in **Figure 5**. Through parameter control, the polymer blends and a block copolymer have a high selectivity of

molecular weight (M_w), crystallinity, and polymer architecture with controlled degradation profiles. Green features such as mild polymerization temperatures and solventless conditions lead to the synthesis of polymer blends and a block copolymer via polycondensation with M_w ranging from 1700 to 2200 g/mol.

Table 4. Overview of DES types, functions, type of polymerization, and their applications in Polymeric Nanomaterials

Type of DES	Function of DES	Type of Polymerization	Applications	Ref.
ChCl/1,2-ethanediol	Solvent for polyaniline (PANI) preparation	Polyaniline (PANI)	Homogenous and denser PANI matrix, 80 – 100 nm PANI fibers, 150 – 250 nm pores.	[123]
ChCl/urea	Solvent for polymerization-induced self-assembly (PISA)	PHEMA-*b*-PMMA spherical particles	Self-assembled PHEMA-*b*-PMMA spherical particles of 60 to 70 nm.	[124-126]
ChCl/itaconic acid (IA)	Solvent for copolymerization of itaconic acid (IA) and N,N'-methylenebisacrylamide (MBA)	Branched copolymers of IA and MBA	Hydrodynamic size ranging from 10 to 100 nm, with 7–9 mol% of MBA.	[127]
ChCl combined with alcohols/ureas	Sol-gel preparation of silica and electrolyte of 1,3:2,4-Dibenzylidene-d-sorbitol (DBS)	Supramolecular eutectogels of DBS	Supramolecular eutectogels for flexible batteries and supercapacitors, self-assembled gels with nanofibrillar morphologies of 20 – 50 nm.	[128]
ChCl/glycerol or monopropylene glycol	Solvent for natural guanosine and H_3BO_3 complexes	Supramolecular eutectogels of natural guanosine and H_3BO_3	Supramolecular eutectogels with G-quadruplex nanowires with diameters less than 100 nm, displaying high ionic conductivity, high thermal stability, excellent injectable properties, and electrochromic activity.	[129]
Acrylic acid (AA) or Methacrylic acid (MAA) with Choline chloride (ChCl)	Polymeric DES system for macroporous PAA-CNxMWCNT composites preparation	Polyacrylic acid (PAA) with N-doped carbon nanotubes (CNxMWCNT)	Macroporous composite materials with homogeneous coating of CNT, 20 – 50 nm morphology.	[130, 131]
Eutectic mixtures of L-lactide and ε-caprolactone with 1,5-Diazabicyclo[4.3.0] non-5-ene (DBN) as catalyst	Polymeric DES system for Ring-opening polymerization (ROP) of L-lactide and ε-caprolactone	Polymer blends and block copolymer of L-lactide and ε-caprolactone	High selectivity of molecular weight (Mw), crystallinity, controlled degradation profiles.	[135]

3.4. Nanomaterials from Biomass

3.4.1. Cellulose

The use of DESs for synthesis of CNC is attracting greater attention due to its countless applications in the current society. The fine tuning of this process has been studied by number of researchers over the time. Among those studies, majority has been conducted using pretreated pulp as the raw material to focus more on the reaction pathway.

A comparison between the conventional approach of using sulfuric acid for size reduction has been conducted by Lim et al. [136]. The team was able to generate CNC from bleached rice straw pulp with a PDI of 0.56 and a zeta potential of value of -52.1 ± 5.2. The main difference observed in this study, apart from the surface chemistry, was the thermal stability of CNC achieved by the DES treatment, in contrast to that of the sulfuric acid treatment, whilst a higher crystallinity index (CRI) of 78.3% gained by the sulfuric acid treatment. A similar comparison with an addition of Fe(III) catalyst (oxalic acid dihydrate:ChCl:FeCl3.6H2O molar ratio of 4:1:0.2) has been conducted by Yang *et al*. where they have obtained CNCs with 5−20 nm diameter and length of 50−300 nm with a CRI of 80-82% [137].

Further, Laitien and coworkers suggested an approach to obtain CNC with a width of 3-8nm and length of 50-350nm by dissolving softwood pulp with choline chloride and oxalic acid dihydrate system as effective stabilizers for oil-water systems [138]. The generation of CNCs using grape pomace from red-winemaking with the use of lactic acid, ChCl system has been studied, where the variation of zeta potential has been observed in grape pomace, brown cellulose, cellulose and CNCs were 9.26 ± 0.25, - 21.95 ± 0.07, - 4.24 ± 3.57 and - 29.07 ±1.66 mV, respectively [139]. The viscosity of the DES plays a major role in particle size reduction applications. In a comparison study between formic acid and urea based DESs, it was observed that the lower viscosity in formic acid-based DES resulted in the production of CNCs of smaller diameters than that of urea based ones [140]. However, in terms of water dispersibility, the surface ester groups generated exhibit more adverse effects due to their inherent hydrophobic nature. Notably, this study reveals a pronounced enhancement in dispersibility within DMAc and DMSO solvents.

The water in DES system plays a vital role in the synthesis of CNC, especially when it comes to fine-tuning the viscosity in the system. The water molecules can facilitate the ionization of H^+ and delocalization of Cl^- in ChCl through the formation of new hydrogen bonds. The addition of 20% water into a DES system containing ChCl/oxalic acid dihydrate has led to a decrease in viscosity from 62 to 1.8 mPa [141]. Even though this change

resulted in some differences in the Kamlet−Taft solvatochromic parameters: slight decrease in (α), 50% decrease in hydrogen bond basicity (β), and slight increase in polarizability (π*) , the team was able to generate CNCs in diameter range of 11-20 nm with CRI of 69.08−70.01%. This approach introduces a scalable method for preparing CNCs using kraft pulp sourced from poplar wood, while maintaining the cellulose crystalline structure with minimal disruption. In this work, the treatment was conducted for one hour at 80°C, employing a 5% fiber loading. Another similar study with the same DES constituents was carried out by Zhang and team. In this work, CNCs were produced within 0.5 hours with the use of high shear rate emulsifier. The team used microcrystalline cellulose with 70 wt% water added to generate CNF with average diameter of 25.1–33.3 nm and a length ranging from 281.3 nm to 404.2 nm [142]. The yield increased by approximately two folds when the treatment time was increased to 2.5hrs. However, this process generated a byproduct of iron (II) oxalate crystals in the mixture owing to the ferruginous stainless steel shear probes in high-rate shear dispersing emulsifiers.

A study carried out by Smirnov *et al.* made an effort to produce CNCs using environmentally friendly DES system of ChCl:urea and was able to generate CNCs with dimensions of 20 x 100 x 700 nm [143]. The treatment had a limited impact on the crystalline regions. A molecular dynamics study conducted on the system unveiled that the reduction in particle size primarily stems from hydrogen bond interactions between cellulose hydroxyl groups, the urea C=O group, and the chloride ions. However, this approach took 2 to 4 days at 110ºC to obtain the desired output. A detailed analysis of the structural transition of bleached cotton fiber using acidic DES (choline chloride/oxalic acid dihydrate) was conducted by Ling and team. Here, the group mainly paid attention on the lattice planes of 1-10, 100 and 200 in cellulose supramolecular structures on hexagonal cross sections (Figure 7a), with DES treatments at different molar ratios at temperatures 80ºC and 100ºC for 2 hours. The authors documented that the esterification effect from oxalic acids was occurring through the hydrophilic (1-10) plane, whereas the disruption of the hydrogen bonding within the glucose molecules happens via the (200) plane and (110) plane. Furthermore, the expansion of d spacings was notably more pronounced at 80°C. Moreover, the combined effect of mechanical disintegration and freeze-drying led to a reduction in crystallinity (from 67.29% to 75.29%) in comparison to bleached cotton cellulose (93.37%).

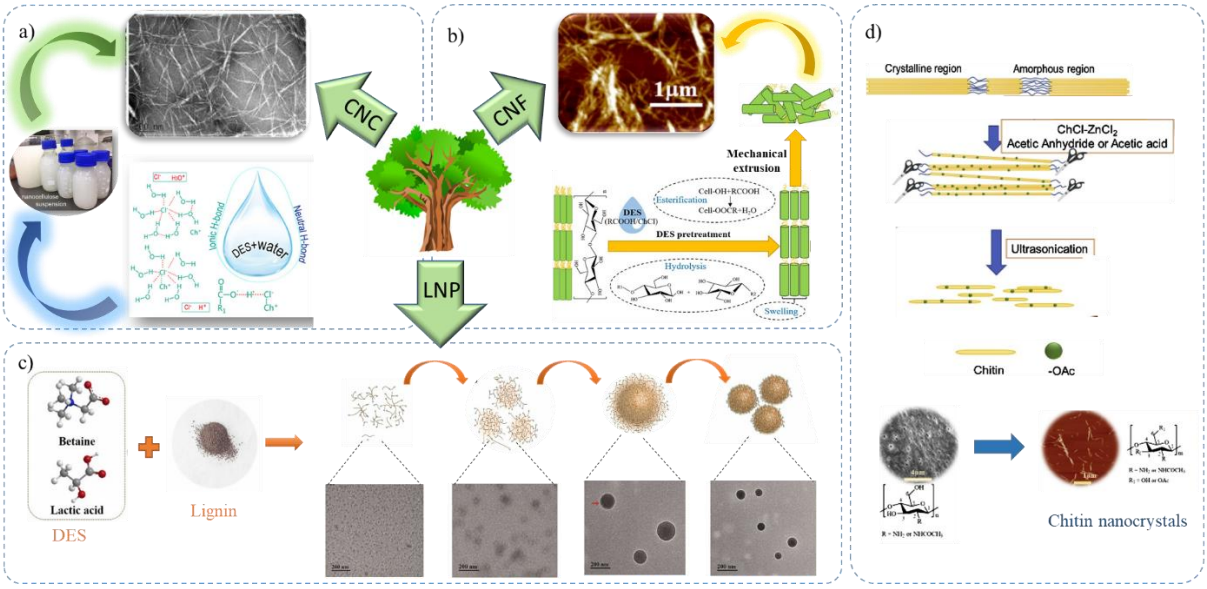


Fig 6. a) Schematic illustration of the formation process of cellulose nanocrystals (CNC), cellulose nanofibers (CNF), lignin nanoparticle (LNP) and chitin nanocrystals (ChNCs). (a) Mass production of CNC using hydrated ChCl/ Oxalic acid dihydrate DES. Reproduced with permission from Ref. [141] Copyright (2019), American Chemical Society. **b)** Preparation of CNF through LA/ChCl pretreatment. Reproduced with permission from Ref. [144] Copyright (2021), Elsevier. **c)** Steps of LNP self-assembly. Reproduced with permission from Ref. [145] Copyright (2022), Elsevier. **d)** Illustration demonstrating the one-step synthesis of partially O-acetylated and esterified ChNCs. Reproduced with permission from Ref. [146] Copyright (2019), Elsevier.

The first synthesis of CNF was reported in 2015 by Sirvio *et al.*, with the use of ChCl/urea DES system at a molar ratio of 1:2. This work has generated CNFs with widths of 2-5 nm and lengths from 15-200 nm [147]. Since then, numerous research studies have been conducted, focusing on the synthesis of CNF from lignocellulosic biomass. This endeavor involves the utilization of diverse combinations of HBAs and HBDs.

A study carried out by Liu and team investigated the esterification of hardwood bleached kraft pulp comparing carboxylic acid-based HBDs (formic acid, lactic acid, acetic acid, malonic acid, oxalic acid, citric acid) [144]. The team was able to produce CNFs with average diameters of 80 nm, with lengths ranging between 6–10 µm with 85ºC treatment. The increase in temperature (up to 100ºC) resulted in further reduction in the diameter ranges (Figure 6b). The comparison between mono, di, and tri carboxylic acids generated CNF diameters from 15- 30 nm, 20- 50 nm, and 10- 25 nm, respectively. The team highlighted three key factors pertaining to cellulose esterification: the propensity for proton release, the capability to disrupt hydrogen bonds, and the stability of

carboxylic acid within DES. In their analysis, they attributed the modification through esterification as beneficial in preventing excessive hydrolysis while concurrently improving the dissolution of cellulose.

Many researchers have employed combinations of acidic pretreatments and mechanical effects for generating CNFs. Yu and coworkers, for example, directly pretreated raw ramie fiber using ChCl and oxalic acid in conjunction with ball milling [148] . The team noted that DES pretreatment significantly enhanced the process efficiency in comparison to exclusive physical treatment, offering the additional benefit of producing CNFs of narrower width (14.29 nm). The impact of introducing excess water has previously been examined in the context of CNC generations [141]. In this study, the transformation from CNF to CNC was accomplished by incrementally augmenting the water content by 10%, 20%, and subsequently by 30%. The microwave-assisted DES pretreatment yielded CNFs with diameters of 20 nm and widths ranging from 300 to 2000 nm. The inclusion of 20-30% additional water was leveraged to generate CNCs.

Another category of acidic DES systems utilized in CNF synthesis involves the incorporation of sulfamic acid as the HBA. Here, the DES plays a dual role by acting as both the and the sulfating agent of the nanoparticles. The unique properties such as soft–soft interaction between ligand and metals and good pH-stability of sulfonated cellulose nanoparticles has attracted distinctive applications in the areas such as water purification [149]. The DES system with sulfamic acid and urea has been studied by Sirvio *et al.* Their study unveiled the production of evenly sized sulfated CNF with a uniform width of 4.4 nm ± 1.6 nm from wood cellulose pulp. The authors attributed this enhancement in property to the elevated charge density inherent within the DES system [149]. An increase in reactivity was noted in tandem with the decrease in urea content, while a reduction in the molar ratio between cellulose and sulfamic acid resulted in a reduction of the polymerization degree of CNF (310-499 as opposed to 545-854). The authors attributed this phenomenon to the inefficient heat transfer caused by the limited amount of liquid sulfamic acid content within the cellulose medium, consequently leading to the pronounced hydrolysis of cellulose.

Another study conducted by Li and colleagues examined the utilization of a DES system consisting of sulfamic acid and glycerol (with a mass ratio of 1:3) for treating bleached kraft poplar pulp at 100°C for a duration of 1 to 1.5 hours [150]. Here, the DES-based swelling led to a high degree of substitution (0.12), and the mechanical grinding generated CNF with diameters between 10 to 25 nm. A reduction of crystallinity (53%) was observed, which was attributed to introduction of sulfate groups.

Further avenues towards the synthesis of cellulose nanoparticles via less hazardous natural DESs has also been studied by several researchers. ChCl and Citric acid-based DES has been employed for the synthesis of CNFs by

Liu and team with high pressure homogenizer for bleached softwood kraft pulp [151]. Two types of citric acids were used for this study namely, anhydrous citric acid and citric acid monohydrate. The CNFs with smallest diameter (17 ± 2 nm), highest zeta potential value (−46.65 ± 4.28mV) and highest carboxyl group content has been achieved by the ChCl:anhydrous citric acid 1:1 molar ratio treated with 100ºC. The generated CNFs indicated better dispersibility in water and higher thermal stability than that of sulfuric acid hydrolyzed CNFs. In a separate study, needle bleached kraft pulp has been used for the synthesis of CNF using eco-friendly ChCl: ethylene glycol DES system (1:1) [152]. Additional physical treatments, encompassing screw extrusion, colloidal milling, and a mild chemical treatment using 0.8wt% H_2SO_4, were incorporated into the system. This multifaceted approach yielded CNC with diameters ranging from 14 to 42 nm. Ethylene glycol was primarily chosen due to its analogous polarity to cellulose and its potential to minimize esterification side reactions. Nevertheless, in this specific study, the authors indicated that the low viscosity did not have a favorable impact on particle size reduction, which was predominantly attributed to the higher polarity of the distilled water.

The progression of hydrogen bonding throughout the nanofibrillation process has been examined through the utilization of a CNF and ChCl-oxalic acid based DES system [153]. In this study, the authors placed an emphasis on understanding the nature of both intra and intermolecular bonding in the presence of DES. They proposed that intramolecular hydrogen bonds, characterized by lower bond energies, exhibited greater susceptibility to substantial bond cleavage during the process. However, when evaluating the sequence of bond cleavage, the observation of O(3)H…O(5) intramolecular H-bond cleavage > O(6)H…O(3′) intermolecular H-bond cleavage > O(2)H…O(6) intramolecular H-bond cleavage was noted. This sequence signified an initial cleavage occurring within the amorphous region, followed by progression towards the crystalline region.

3.4.2. Nanolignin

Lignin nanoparticles (LNP) is another class of material with high value in material synthesis. These materials are generated from lignocellulose biomass, which are known for their desirable properties including antioxidant, UV barrier and compelling mechanical properties. The synthesis of LNPs do not involve high level of mechanical disintegration as compared to the synthesis of cellulose-based nanoparticles. In many instances, the approach involves DES treatment-based dialysis coupled with self-assembly, as observed in most application [154, 155]. In this type of reactions, the cleavage of β-O-4 linkages is mainly expected, along with other bond cleavage such as, β-β, β-5, etc. [156]. Additionally, the self-assembly of LNP through π–π stacking interactions also plays a major role [145, 157, 158]. Here, the scope of these studies extends beyond acidic DES to encompass alkaline and neutral DES systems as well.

The synthesis of LNPs using corncob has been studied by Zhang *et al.* using ChCl-lactic acid-based DES system which yielded self-assembled LNPs with a high yield (85.6%) and high purity (97.8%). A hydrodynamic diameter of 48.66 nm has been achieved with PDI below 0.2 and zeta potential values exceeding -42.2 mV. The study was conducted by varying the molar ratios, reaction temperatures and reaction time. The authors concluded that temperature played a pivotal role in generation of LNPs [145]. Yan *et al.* conducted a DES treatment on rice straw using a ternary DES system consisting of ChCl, oxalic acid, and lactic acid in a ratio of 1:0.5:1. This treatment was performed with microwave irradiation (680 W) for a duration of 4 minutes. In this work, the authors highlighted on the high rate of lignin removal within the range of 60.8%–63.4%, as opposed to a binary DES system only with 7.6%–9.6% yield [157].

Zhang *et al.* conducted an exhaustive investigation into the self-assembly of LNPs through water dropping. They employed betaine:lactic acid (1:2) as the system, subjecting it to a treatment lasting 12 hours at room temperature (25ºC), followed by a subsequent 72-hour dialyzing step [145]. The authors noted a structural transition in lignin as water is added into the system, progressing from a solution state to the formation of local clusters and irregular particles, ultimately culminating in the creation of stable colloid spheres with an average size of 57.16 ± 1.43 nm (Figure 6c). In the study, a comparison between lignin starting material and LNPs was carried out. Improved thermal stability (378.16ºC), higher antioxidant activity, and a lower minimum inhibitory concentration against *Staphylococcus aureus* was observed in the LNPs.

Acidic DES pre-treatments have been used to valorize lignocellulosic biomass, resulting in the generation of several valuable products such as LNPs, LCNFs, activated nano carbons, and carbon quantum dots at various stages. The evaluation of the effects of these specific steps on the production of LNPs was also reported [156, 158, 159]. In these studies, the hydrothermal pre-treatments were carried out at high temperature (approximately 170ºC) prior to DES treatments. The pre-extraction of hemicelluloses leads to reduction of the molecular weight of the biomass facilitating the generation of LNPs [156]. Tian and team studied a variety of lignocellulose biomass including poplar wood chips, pine wood shavings, moso bamboo powder, wheat, and rice straw. DES pre-treatment of these lignocellulose biomass generated nanomaterials viz, activated nanocarbons, LCNFs and LNPs using ChCl-lactic acid (1:2) [158]. The pre-treatment generated LNPs with particle size ranging 200-600 nm, where pine wood shavings based LNPs indicated the smallest size with lowest PDI. The comparison of LNPs generated from different biomasses revealed that higher number of hydrophilic groups (i.e. total phenolic OH and COOH) lead to the formation of larger particles, whereas high number of aliphatic OH groups resulted in smaller particle sizes. Xu and colleagues conducted a microwave-assisted pre-treatment utilizing the same DES constituents in a

molar ratio of 1:9, employing bamboo powder as the substrate. They emphasized that the in-situ reactions, including esterification, condensation, and cleavage, acted on lignin, enhancing its amphiphilicity which drives the self-assembly of LNPs [159]. In another work, Ma and colleagues investigated the Lewis acid catalyzed DES pretreatment of abaca, employing a mixture of ethylene glycol, ChCl, and aluminum chloride at a molar ratio of 2:1:0.1. This approach involved a relatively short treatment duration (30 minutes) at 100°C, yielding an optimal output characterized by a size range of 30-50 nm [160]. This process also induced a reduction in molecular weight compared to the initial material (from 7,520 to 1,640), coupled with a reduction of the PDI from 2.21 to 1.29.

Alkaline DES has been adopted for LNPs synthesis due to its specific advantages over both acidic and neutral DES treatments. In comparison to acidic DES, alkaline DES is advantageous in facilitating condensation reactions that elevate molecular weight. Moreover, when compared to neutral DES treatments, alkaline DES stands out for its relatively lower pre-treatment efficiency [155]. The effect of ChCl-ethanolamine treatment (1:6) along with the incorporation of 1wt% and 3wt% corncob alkali lignin biomass resulted in the synthesis of LNPs within the size range of 8.9 to 64.9 nm, respectively. Remarkably, these LNPs demonstrated the capability to maintain their size stability over a period of 30 days [154]. In another study utilizing the same DES system, the stability of LNPs in a water medium was observed. The study involved kraft lignin powder for the preparation of alginate-based gel beads for the purpose of removing methylene blue from water [161]. Another class of alkaline DES (K_2CO_3 and glycerol, 1:5) has been utilized by Yue and coworkers. Their approach involves the tuning of the pH of the solvent to 2, 4, and 6 to investigate the self-assembly of LNPs [155] using wheat straw. Here, the team observed that the lignin fractioned at lower pH (i.e., pH 2) displayed uniform and well-shaped particles (600-700 nm) with zeta potential ranging from -38 to -51 mV, and highly stable over 90 days.

All in all, it is evident that extensive efforts have been made to utilize DESs for the reduction of the particle size in lignocellulose biomass. Gaining a comprehensive understanding of the DES system's physical properties, including viscosity and density, as well as delving into its chemical aspects, such as bonding nature and interactions within the biomass, is essential. In addition, the understanding of pre-treatment conditions applied to the biomass, encompassing factors like temperature, pressure, mechanical actions, and the drying method, in tandem is crucial for efficiently synthesizing lignocellulose-based nanoparticles. Nevertheless, there remains plenty of opportunities for future research. These encompass the use of alternative DES combinations, beyond the typical ChCl as HBA. Further avenues include a more comprehensive exploration of Type V DES for particle size reduction, and the innovation of energy-efficient methodologies across the entire process. Such undertakings stand poised to elevate sustainability and broaden the horizons of nanoparticle synthesis.

3.4.3. Nanochitin

Chitin, a biopolymer from marine biomass like crustacean shells, holds great potential for producing nanomaterials due to its biocompatibility, biodegradability, and versatility. However, efficient and eco-friendly extraction is challenging. Recently, DESs have emerged as a promising alternative, offering an effective solvent system for chitin extraction. This approach opens new possibilities for developing nanochitin with diverse applications, and recent research highlights advancements in DES-based extraction methods.

A research done by Mukesh *et al.*, DESs have been employed as solvents for the synthesis of chitin nanofibers (ChNFs) with promising results [162]. DESs composed of the mixture of choline chloride and thiourea (CCT 1:2) were found to be effective in producing ChNFs with diameters ranging from 20 to 30 nm. However, DESs containing urea (CCU 1:2) as the hydrogen bond donor did not yield nanofibers. A comparison was made between the physicochemical properties of the ChNFs obtained using DESs and those obtained using imidazolium-based ionic liquids and choline-based bio-ionic liquids. The ChNFs obtained using DESs as solvents were further utilized to prepare calcium alginate bio-nanocomposite gel beads, which exhibited enhanced elasticity compared to conventional calcium alginate beads. Moreover, these bio-nanocomposite gel beads demonstrated the ability to achieve controlled release of 5-fluorouracil, an anticancer drug, under physiological conditions (pH 7.4). The findings of this study indicate that DESs, particularly the mixture of choline chloride and thiourea, are suitable solvents to produce chitin nanofibers. Furthermore, the prepared ChNFs showed potential for applications as reinforcement fillers in calcium alginate-based systems, offering improved mechanical properties and controlled drug release capabilities. These results highlight the potential of DESs in nanomaterial synthesis and their relevance in developing advanced biomaterials for various biomedical applications.

In a more recent study, Hong *et al.* successfully developed a novel method for the one-pot production of acetylated and esterified chitin nanocrystals with rod-like morphology [146]. The use of choline chloride-zinc chloride deep-eutectic solvent (ChCl-$ZnCl_2$ DES) as the reaction solvent and catalyst allows for simultaneous acetylation, esterification, and hydrolysis of chitin, resulting in chitin nanocrystals (ChNCs) with lateral dimensions ranging from 20 to 80 nm in width and 100 to 700 nm in length (Figure 6d).

The obtained ChNCs exhibited intact chemical structures and offer great potential for various applications in nanotechnology and materials science. However, the thermal stability of the ChNCs decreased after treatment with ChCl/$ZnCl_2$, and CNCs functionalized with acetic acid exhibited lower thermal stability compared to those functionalized with acetic anhydride. Notably, the ChCl-$ZnCl_2$ DES demonstrated low expenditure and toxicity,

highlighting its potential as a green and environmentally friendly solvent to produce functional chitin nanocrystals. This DES-based approach offers a promising and sustainable route for the one-step functionalization of chitin to obtain tailored ChNCs.

The same group also investigated using DES derived from ferric chloride hexahydrate and betaine chloride in a molar ratio of 1:1 was employed as a hydrolytic medium to ChNCs with high yield (up to 88.5%) [163]. The unique combination of Lewis acid from ferric chloride and Brønsted acid released from betaine hydrochloride enabled the efficient hydrolysis of chitin, facilitated by ultrasonication with low energy consumption. The resulting ChNCs exhibited an average diameter of 10 nm, length of 268 nm, and a crystallinity of 89.2% under the optimal synthesis conditions (chitin-to-DES mass ratio of 1:20, at 100 °C for 1 hour). The ChNCs demonstrated promising potential as efficient emulsion stabilizers. Even at a high oil content of 50%, stable oil-in-water (o/w) emulsions were achieved with a low dosage of ChNCs (1 mg/g). Importantly, the DES treatment preserved the chemical structure of ChNCs while enhancing their crystallinity by removing the amorphous parts of chitin. Additionally, the thermal stability of the ChNCs obtained using this method was comparable to that of pristine chitin, enhancing their potential for use in thermoplastic applications. This study successfully prepared ChNCs using a ferric chloride and betaine hydrochloride DES, achieving excellent yield and stability. The ChNCs show promise as green, non-toxic emulsion stabilizers for industries like food and cosmetics. DES-based production presents a sustainable, efficient alternative to conventional methods, expanding their potential applications.

In a study done by Yuan *et al.*, five different acidic deep eutectic solvents (DESs) composed of choline chloride and organic acids were utilized for the fabrication of ChNCs [164]. The DESs demonstrated excellent performance in producing high-quality ChNCs with high mass yields ranging from 78% to 87.5% under optimized reaction conditions. These acidic DESs played a dual role in the fabrication process, promoting the hydrolysis of chitin while also serving as an acylation reagent. The physicochemical characterization of chitin revealed that the DES treatments resulted in the removal of amorphous areas, leading to increased crystallinity of the ChNCs. The dimensions of the ChNCs varied depending on the specific DES used, with average diameters ranging from 42 nm to 49 nm and lengths ranging from 257 nm to 670 nm. Importantly, the thermal stability of the ChNCs was comparable to that of pristine chitin, indicating their suitability for various applications. In summary, the acidic DES systems presented a simple, effective, and environmentally friendly method for the one-step production of O-acylated chitin nanocrystals. Their ability to produce high-quality ChNCs with desirable properties makes them a promising option for various applications in nanomaterials and beyond.

A recent review done by Li *et al.* summarizes how DESs exhibit remarkable potential for pre-treating chitin to produce chitin nanomaterials. Acid-based DESs remove the amorphous region of chitin, while non-acid-based DESs retain it [165]. Subsequent mechanical disintegration yields ChNCs and ChNFs with distinct yield, morphology, and surface chemistry. Despite the advantages of DESs over conventional solvents, several challenges remain. Cost-effectiveness is a concern due to the high mass ratio of DESs to chitin required for extraction. Additionally, further efforts are needed to enhance the recyclability of DESs and evaluate their environmental impact. Future directions include optimizing DES chemical structure, developing efficient DES recovery and purification methods, and conducting life cycle assessments.

These studies highlight the potential of DESs in processing chitin for nanomaterial development, producing ChNFs and ChNCs with properties like controlled drug release, enhanced elasticity, and emulsion stability. Challenges remain in cost-effectiveness, recyclability, and environmental impact. Future efforts will focus on optimizing DES structures, improving recovery methods, and assessing life cycle impacts. With advancements, DESs could replace traditional solvents for sustainable chitin-based nanomaterial production. Table 5 summarizes the DES types, biomass, nanomaterials, and processing techniques.

Table 5. Overview of the types of DES, types of biomasses, nanomaterials, treatments or methods, and the produced nanomaterials from biomass

Type of DES	Type of Biomass	Type of Nanomaterial	Nanomaterial Produced	Ref.
ChCl/oxalic acid dihydrate	Rice straw pulp	CNC	CNC with PDI of 0.56, zeta potential of -52.1 ± 5.2, and thermal stability	[136]
ChCl/oxalic acid dihydrate + Fe(III) catalyst	Bleached eucalyptus kraft pulp	CNC	CNCs with 5−20 nm diameter, CRI of 80-82%	[137]
ChCl/oxalic acid dihydrate	Softwood pulp	CNC	CNC with width of 3-8 nm, length of 50-350 nm	[138]
ChCl/lactic acid	Grape pomace (red wine)	CNC	CNCs with variation in zeta potential	[139]
Formic acid-based	Not specified	CNC	CNCs of smaller diameters than urea-based DES	[140]
ChCl/oxalic acid dihydrate	Kraft pulp (poplar wood)	CNC	CNCs in diameter range of 11-20 nm, CRI of 69.08−70.01%	[141]
ChCl/oxalic acid dihydrate	Wood pulp or cotton pulp	CNF	CNF with average diameter of 25.1–33.3 nm	[142]
ChCl/urea	Not specified	CNC	CNCs with dimensions of 20 x 100 x 700 nm	[143]
ChCl/urea	Raw cotton fiber	CNF	CNFs with widths of 2-5 nm and lengths from 15-200 nm	[147]
Various carboxylic acid-based HBDs	Hardwood bleached kraft pulp	CNF	CNFs with average diameters of 80 nm, lengths ranging between 6–10 μm, and varied diameters for mono, di, and tri carboxylic acids	[144]
ChCl and oxalic acid	Raw ramie fiber	CNF	CNFs with narrower width (14.29 nm) and enhanced efficiency	[148]
Sulfamic acid-based	Wood cellulose pulp	Sulfated CNF	Sulfated CNF with uniform width of 4.4 nm ± 1.6 nm from wood cellulose pulp	[149]
Sulfamic acid and glycerol	Bleached kraft poplar pulp	CNF	CNFs with diameters between 10 to 25 nm and reduction in crystallinity (53%)	[150]

ChCl/citric acid	Bleached softwood kraft pulp	CNF	CNFs with smallest diameter (17 ± 2 nm), highest zeta potential value, and high carboxyl group content	[151]
ChCl/ethylene glycol	Needle bleached kraft pulp	CNC	CNCs with diameters ranging from 14 to 42 nm	[152]
ChCl-oxalic acid	Softwood kraft pulp	CNF	Understanding the progression of hydrogen bonding throughout the nanofibrillation process	[153]
ChCl, oxalic acid, and p-toluenesulfonic acid	Thermomechanical pulp	LCNCs	LCNCs with a width of approximately 6 nm and a thickness of 3.3 nm, high thermal stability, 47.8% lignin content, and a yield of 66%	[166]
Lactic acid-based	Energy cane bagasse	LCNFs	LCNFs with 81% delignification, average crystal size ranged from 3.14±0.01 nm to 3.44±0.02 nm, crystallinity of 71.2%, and improved UV stability	[167]
ChCl with formic acid, lactic acid, acetic acid	Corncobs	LCNFs	LCNFs in the diameter range of 60–90 nm with enhanced re-dispersibility in organic solvents	[168]
ChCl/lactic acid	Hardwood bleached kraft pulp	LCNFs	Production of LCNFs with diameters measuring less than 100 nm	[169]
ChCl/ethanolamine	Corncob alkali lignin	LNPs	LNPs within the size range of 8.9 to 64.9 nm, size stability over 30 days	[154]
K_2CO_3/glycerol	Wheat straw	LNPs	Uniform particles (600-700 nm) with zeta potential ranging from -38 to -51 mV, highly stable over 90 days	[155]
ChCl, oxalic acid, and lactic acid	Rice straw	LNPs	High rate of lignin removal (60.8%–63.4%), yield of 7.6%–9.6%	[157]

ChCl/lactic acid	Corncob	LNPs	Self-assembled LNPs with a high yield (85.6%) and high purity (97.8%), hydrodynamic diameter of 48.66 nm, PDI below 0.2, and zeta potential exceeding -42.2 mV	[145]
Betaine/lactic acid	Corncob	LNPs	LNPs with an average size of 57.16 ± 1.43 nm, improved thermal stability, higher antioxidant activity, and lower minimum inhibitory concentration against Staphylococcus aureus	[145]
ChCl/lactic acid	Poplar wood chips, pine wood shavings, moso bamboo powder, wheat, rice straw	LNPs	LNPs with particle size ranging 200-600 nm, size influenced by the number of hydrophilic and aliphatic OH groups	[158]
ChCl/lactic acid (microwave-assisted)	Bamboo powder	LNPs	Drives the self-assembly of LNPs	[159]
ChCl, aluminum chloride, and ethylene glycol (Lewis acid catalyzed)	Abaca	LNPs	LNPs with a size range of 30-50 nm, reduced molecular weight and PDI	[160]
Choline chloride/thiourea	Crab shells	ChNFs	ChNFs with diameters ranging from 20 to 30 nm	[162]
Choline chloride/zinc chloride	Shrimp shells	ChNCs	ChNCs with lateral dimensions ranging from 20 to 80 nm in width and 100 to 700 nm in length	[146]
Ferric chloride/betaine chloride	Shrimp shells	ChNCs	ChNCs with an average diameter of 10 nm, length of 268 nm, and 89.2% crystallinity	[163]
Choline chloride/organic acids (varied)	Crab shells	ChNCs	ChNCs with mass yields ranging from 78% to 87.5%, dimensions varying by specific DES used	[164]

Urea/Guanidine hydrochloride (PD-DES)	Silk fibres	Silk Nanofibrils (SNFs)	SNFs with diameters of 20-100 nm, lengths of 0.3–10 μm. Membranes with nanoporous structure, high mechanical strength, and thermal stability. Capacitance: 171 F g^{-1}.	[170]
Amino acids/D-sorbitol (renewable DES)	Silk fibres	Silk Nanofibrils (SNFs)	SNFs with preserved crystalline structure. Nanocomposite membranes with enhanced mechanical strength (416.7 MPa) and thermal conductivity (3.84 $W \cdot m^{-1} \cdot K^{-1}$)	[171]

4. Applications of DES-synthesized nanomaterials

Due to the exceptional properties of DESs, compared to ionic liquids or organic solvents, DESs or DES-synthesized nanomaterials have found potential applications in many sectors, as depicted in **Figure 7.**

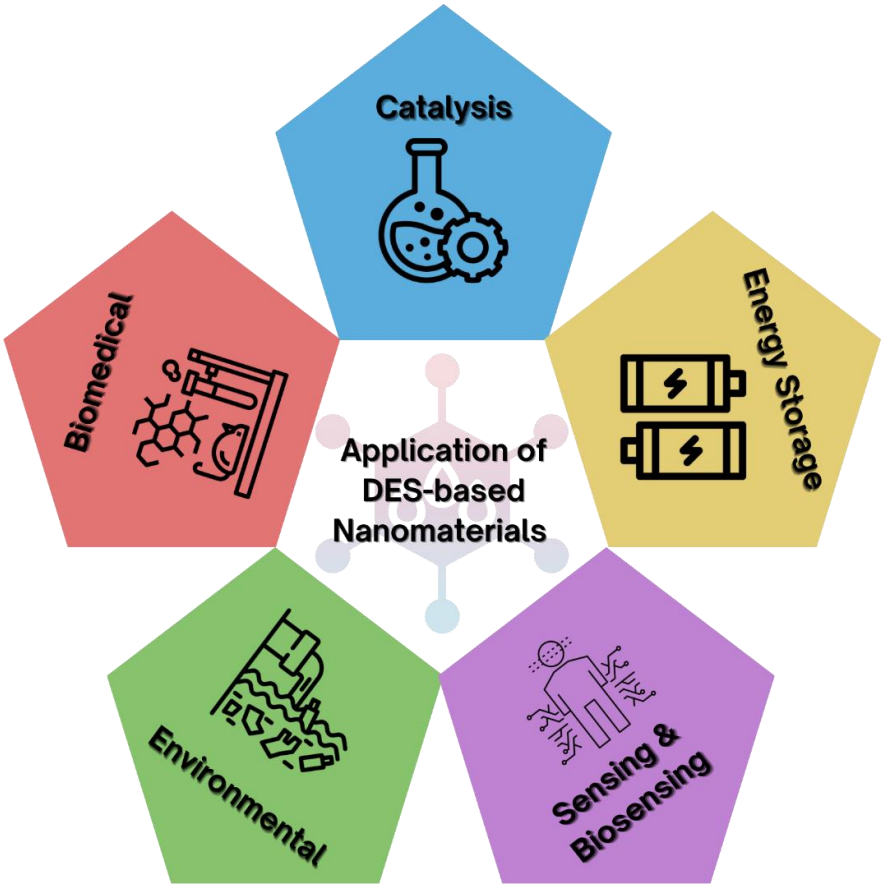


Fig 7. Various potential applications of deep eutectic solvents (DES)-synthesized nanomaterials.

4.1. Catalysts

Nanomaterials synthesized using DES as a precursor or template can exhibit unique catalytic properties. These materials can be employed as effective catalysts in a variety of chemical reactions, including oxidation and carbon dioxide reduction, due to their large surface area, regulated shape, and improved stability. Beyzavi and colleagues [172] prepared a recyclable catalyst consisting of a covalently immobilized deep eutectic choline chloride/p-toluenesulfonic acid (*pTSA*) solvent for the chemoselective direct *ipso*-etherification and amination of naphthols from magnetic nanoparticles (MNPs). The binding of DES to the nanoparticle surface resulted in the enhanced catalytic activity and facilitated the catalyst recovery from the catalytic waste product mixture. The results showed that the average size of the MNP-bound DES particles was 122 nm. Using a functionalized magnetite nanoparticle catalyst for etherification and amination, average yields were 84 and 77%, respectively. The catalytic efficiency

was ascribed to the homogenous nanoparticle distribution, robust DES-support, and hydrogen-donating interplay with naphthols. This study provides an overview of catalytic PDES covalently linked to MNPs as a model for organic reactions.

Other studies have also demonstrated the catalytic potential of DES-based nanomaterials across various applications. For example, Fe_3S nanostructures synthesized via a DES solvothermal method exhibited high efficiency in electrochemical nitrogen reduction [173], while high-entropy metal phosphides (HEMPs) produced using DESs proved effective for water splitting [174]. DESs also enabled the scalable synthesis of g-C_3N_4/metal oxide composites, significantly boosting nitrogen photocatalysis [175]. Additionally, high-entropy metal–organic frameworks (HE-MOFs) synthesized in DESs displayed enhanced electrocatalytic activity for oxygen evolution [176]. In biomass conversion, DES-derived NiS_2/CdS nanospheres efficiently catalyzed the transformation of 5-hydroxymethylfurfural to valuable chemicals under visible light [177]. These works highlight the versatility of DESs in improving catalytic performance for sustainable chemical processes.

4.2. Energy storage applications

DES-based nanomaterials have shown promise in energy storage applications. For example, DES-derived carbon nanomaterials have been used as electrode materials for supercapacitors and batteries and exhibit high specific capacitance and improved electrochemical performance. Kim *et al.* [178] designed a Z-scheme heterojunction catalyst by deposition of uniform copper (II) oxide nanoclusters on TiO_2 surface mediated by choline chloride and urea (1:2 M ratio) DES. The fabricated Z-scheme heterojunction, formed by surface interactions of Cu_2O nanoclusters and TiO_2 nanoparticles, improves the photogenerated charge carrier separation. In addition, the Cu_2O/TiO_2 heterojunction surface chemical treatment resulted in oxygen vacancies due to defects creation during in situ Cu_2O synthesis. The final Cu_2O/TiO_2 catalyst has a higher electric charge per unit volume coupled with about 238 % a lower charge transfer resistance in relation to $6.3 \times 10^{19}/cm^3$ of pure TiO_2. More importantly, the optimized Cu_2O/TiO_2 photocatalyst had about 132% higher H_2 production rate than neat TiO_2 (~1.83×10^{-2} µmol g^{-1} h^{-1}). The use of DESs-assisted fabrication of photocatalyst from mono-sized Cu_2O nanoclusters on TiO2 underscores a critical shift in photocatalytic hydrogen production. In another study, Hammond *et al.* \[98] studied the in situ formation of iron oxide nanoparticles (hematite) in choline chloride: urea media. The separation of Fe^{3+} in DES solution was determined by extended X-ray absorption fine structure and the atomic structure of the alloy was determined by neutron and X-ray diffraction and empirical potential structure refinement modelling. The results showed that the iron salts formed $[Fe(L_{)3}(Cl)_3]$ octahedral complexes. where (L) represents various O-containing ligands. Dissolved Fe caused unusual structural reorganizations in DES due to chloride removal from

the complex and alteration of hydrogen bonds around the complex. Extended X-ray absorption fine structure (EXAFS) suggests that these complex forms [OFeO] oligomers with pseudo zero-order kinetics upon reaction of urea with the thermal hydrolysis products of iron. In hydrated DES, nuclei formation and growth constitute a rapid reaction, whereas in pure DES the initial rate was rapid but dropped within 90 minutes. By creating nanostructured thin films of the hematite nanoparticles, its performance as an anode for splitting water into hydrogen using sunlight will be improved. Other materials have been synthesized such as copper–zinc–tin chalcogenide (Cu_2ZnSnS_4CZTS) [179] for energy storage, activated carbon decorated-NiO (NiO/AC) for hydrogen fuel [180], gold nanoparticles for electrocatalysis [181], and nanoferrites as magnetic storage devices [182]. Notably, machine learning models are increasingly used to accelerate the discovery of DESs for nanomaterials synthesis. A Conditional Generative Adversarial Network (CGAN) was developed to predict cathode solubility in DESs, significantly speeding up the identification of promising candidates [183]. Combined with XGBoost, these models offer high accuracy and efficiency, streamlining DES development for applications like lithium-ion battery recycling.

4.3. Sensing and Biosensing applications

Nanomaterials made from DES offer enhanced sensing capabilities. Functionalized nanoparticles can be synthesized using DES as a solvent, enabling the fabrication of sensitive and selective analyte-recognition detector, including heavy metals, gases, biomolecules and food analysis [184]. Brett and colleagues [185] fabricated polymerized films of brilliant cresyl blue (PBCB) by electrodeposition on carbon nanotube-modified glassy carbon electrodes by potential swings in ethaline (choline chloride + ethylene glycol) with the inclusion of various ions. The PBCB nanocomposite films synthesized at 150 mV/s in ethaline + NO_3^- showed higher electrochemical activity. Moreover, the PBCB/Ethaline-HNO_3/MWCNT and $PBCB_{aq}$/MWCNT films acted as electrode supports in glucose and catechol biosensing by glucose oxidase and tyrosinase enzymes, respectively. Row and Li [186] prepared hexagonal boron nitride (h-BN) polymer nanoparticles in DES via molecular recognition technology. In their work, they produced the molecularly imprinted polymers by presenting the h-BN as a 2D sheet. These MIPs were obtained either from DES or DES/h-BN mixture with a crosslinker (ethylene glycol dimethacrylate), an initiator (AIBN), a porogen (methanol), and a template (quercetin). The binding site of the monomer was protected by DES hydrogen bonding before MIP polymerization. The introduction of h-BN increased the surface area of the formed MIP nanoparticles. These nanoparticles were used as solid-phase extraction adsorbents to extract flavonoids from ginkgo biloba leaves. In comparison with the conventional MIP nanoparticles, the new sorbent shows a significantly improved detection ability for flavonoids.

In another work, Boczkaj and colleagues [187] prepared silver nanoparticles (Ag-NPs) in conjunction with deep eutectic solvent (DES) of choline chloride: phenol (1:2) in a wet chemistry approach. They observed a synergistic effect in nanoparticles-DES interactions during extraction of lead from edible oils through sonochemistry. They further characterized the purified edible oil using flame atomic absorption spectroscopy (FAAS). Notably, the system showed excellent detection limit (DL) and limit of quantification (LOQ) of 0.28 µg/L and 0.94 µg/L, respectively. The Ag-NPs-DES system is therefore suitable for Pb(II) ions detection and analysis in edible oil and other foods to promote food safety. In another work, Smirnov's group [143] prepared nanocellulose (CNC) using deep eutectic solvents (DES). The choline chloride: urea DES was used to dissolve microcrystalline cellulose at 110°C for 2-4 days, and then redispersed to form highly crystalline CNC of 20 nm in diameter. The authors used a computer model to decipher the dissolution mechanism and found that interactions of hydroxyl and carbonyl groups of cellulose and urea, respectively, and chloride ions are key factors in the dissolution process. Result showed that the dissolution process of DES did not affect the stability of the stable cellulose crystalline structure (Iβ) with crystallinity of about 80 %. Furthermore, the resultant 2 wt.% CNC was used to produce DES- plasticized chitosan film with high strength (~20.4 MPa) and elongation of about 90%. These resultant films could be applicable in functional food packaging. Other notable works on synthesis of gold nanoparticles in DES for biomedical sensors [87, 188].

4.4. Environmental Applications

Nanomaterials derived from DES can play a crucial role in environmental remediation. For example, DES-based nanomaterials can be used environmental bioremediation e.g. heavy metals and organic pollutants removal from water and soil due to their high adsorption capacity and selective binding properties [189]. For instance, Xu *et al.* [190] synthesized a group of DESs using caprolactam as HBD and halide quaternary ammonium salts as HBA. Among the different halide quaternary ammonium salts and different molar ratios of HBD and HBA, tetrabutylammonium bromide/caprolactam (TBAB/CPL = 1:2) was found superior in sulfur removal efficiency with a distribution constant (K_{pc}~5), which was almost much higher than the metal-free DES of IL. Notably, sulfur removal efficiency could reach 96.6% after two-steps separation. Finally, the authors systematically investigated the removal method using 1H NMR and IR spectroscopy. The greater desulfurization efficiency was ultimately attributed, according to investigations using density functional theory, to hydrogen bonding and CH interactions between DES and dibenzothiophene which enabled effective removal of dibenzothiophene from model fuels. The results resonate well with the concerted efforts for production of low-sulfur diesel fuels to cut on carbon emissions equivalents of sulfur oxides.

In another work, Pedrazzo *et al.* [191] fabricated β-CD nanosponges from β-cyclodextrin in type V DES of choline chloride and citric acid using mechanochemistry approaches as shown in Figure 8a. The authors first prepared the NADES by mixing 1:1 molar of components, then obtained β-CD-based polymer using ball milling (BM) and extrusion (TSE). For ball milling, the mixture of β-CD, citric acid, choline chloride, and sodium hypophosphite monohydrate (catalyst) were charged into the jar with zirconia balls and rotated for 4h/30 min intervals to recover a white paste. On the other hand, the same mixture was extruded at 110°C/4h at a speed of 80 rpm to obtain a dark yellow–green paste. The resultant β-CD-based polymers from BM and TSE were water soluble without crosslinking and insoluble after crosslinking. These β-CD-based polymers processed using mechanochemistry could find applications in the environmental sectors. In application of β-CD nanosponges in light rare earth elements (Cerium and lanthanum) removal from wastewater, Badawi *et al*. [192] showed that their efficient adsorption of Ce and La with capacities of about 625.34 and 773.29 mg g^{-1}, respectively. As shown in Figure 8a, the solution temperature significantly impacted the density of functional groups involved in the adsorption of La and Ce ions, likely due to changes in these groups during the adsorption process.

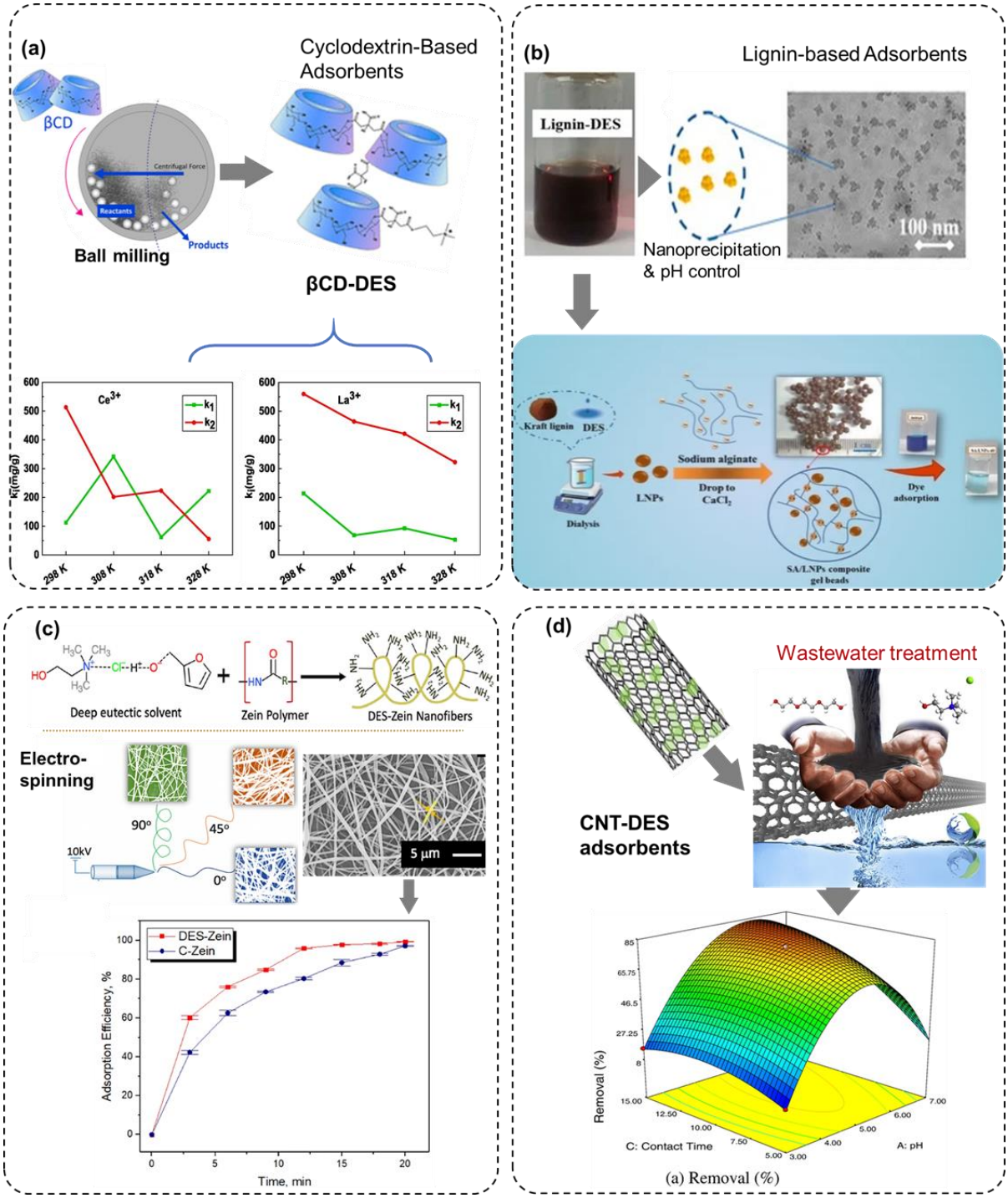


Fig 8. Fabrication of various adsorbents using DES for environmental applications (a) cyclodextrin-based adsorbents via ball milling method. Reproduced with permission from Ref.[191] Copyright (2021), American Chemical Society and adsorption of light rare earth elements using β-CD nanosponges. Reproduced with permission from Ref. [192] Copyright (2023) Elsevier; (b) nanoprecipitation of lignin-based adsorbents. Reproduced with permission from Ref. [193], and formation of LNP/sodium alginate gel beads for methylene blue adsorption. Reproduced with permission from Ref. [194]; (c) electrospun zein-based nanofibers and dye removal efficiency of DES-Zein nanofibers and conventional-Zein. Reproduced with permission from Ref. [195];

(d) carbon nanotubes adsorbents for wastewater treatment and the surface response pattern of the interaction between pH and adsorbent dosage for the removal of Pb(II), Reproduced with permission from Ref. [196] Copyright (2016), Elsevier.

DESs have found applications in lignocellulosic treatment and extraction [194, 197, 198]. For instance, Lyu *et al.* [193] employed nanoprecipitation technique to prepare uniform lignin nanoparticles (LNPs) in DES. In their work, they dissolved lignin in various DESs and then produced higher yield of self-assembled LNPs by nanoprecipitation as depicted in Figure 8b. The resultant LNPs had outstanding dispersibility and excellent long-term stability and diameters of about 20-200 nm dictated by DES type. For instance, choline chloride: ethylene glycol (1:2) DES resulted in LNPs of 30.4 nm. The mechanism of LNPs formation was elucidated as diffusion-limited cluster–cluster aggregation (DLCA). This ecofriendly process of regenerating LNPs from DES/lignin solution using water as a non-solvent is not only facile, but also advances lignin-based nanotechnology for applications in personal care products, energy storage, and environmental cleanup. For instance, gel beads have been created by mixing LNPs with sodium alginate (SA) and their ability to adsorb methylene blue (MB) has been proven as shown in Figure 8b [194]. Kim *et al.* [195] fabricated zein nanofibers using deep eutectic solvent comprising of choline chloride: furfuryl alcohol (1:2 M ratio)(DES-zein) by electrospinning technique (Figure 8c) The optimum 45% (w/w) DES-zein concentration at neutral pH, exhibited an electrical conductivity value of 233 mS/cm. The nanofibers derived from DES-zein solution showed a tweed-like cedar leaf features tuned from different angles. Furthermore, DES zein nanofibers showed a superhydrophilic character in relation to the hydrophobic conventional zein nanofibers, and with 200 nm size in average diameter. This zein nanofibers fabrication method using DES unlocks the potential of continuous electrospinning of fibers with tunable morphology and could be useful in environmental applications. For instance, DES-Zein nanofibers had a rapid adsorption of about 80% of dye within 5 minutes while conventional Zein nanofibers (C-Zein) nanofibers had a slower removal rate of 60%.

Deep eutectic solvents (DESs) are emerging media for the fabrication and application of carbon nanomaterials [199]. In this regard, AlOmar *et al*. [196] synthesized various DESs derived from choline chloride and various hydrogen bond donors (HBDs) as shown in Figure 8d. Subsequently, carbon nanotubes (CNTs) were modified using as-prepared DESs for use as chemosorptive material for pollutants from water, especially, lead ions. The modified CNT adsorbents with triethylene glycol (TEG-CNTs) recorded about 94.7% removal rate for Pb(II), and an optimal adsorption capacity (Q_{max}) of about 288.4 mg/g. Moreover, the impact of pH and contact time on Pb(II)

removal revealed that the percentage adsorption increased over time, peaking at pH 5, and then decreasing as the pH increased. These modified CNT nanomaterial in DES are particularly important in wastewater treatment.

4.5. Biomedical applications

DES-based nanomaterials can be used in drug delivery systems for the controlled and targeted release of therapeutics. The unique physicochemical properties of DES, combined with the ability to encapsulate drugs in nanomaterials, allow for efficient drug delivery, enhanced solubility, and sustained release profiles.

For instance, Ling's team [200] fabricated and examined two types of cellulose nanomaterials as energy conversion surfaces to enable colorimetric detection of human neutrophil elastase (HNE) and various inflammatory disorders. In their work, they used a eutectic mixture derived from choline chloride: oleic acid (1:3 M ratio) to facilitate cotton cellulose nanocrystals (DCNCs) formation, and for the preparation of peptide-cellulose conjugate as a protease sensor from HNE. Notably, DCNCs not only highly substituted HNE tetrapeptide but also had greater sensitivity to elastase than the TEMPO-oxidized wood cellulose nanofibrils (WCNFs). Moreover, structural character of DCNCs revealed crystallinity was high with larger crystallite sizes and the cellulose chains were well-aligned for binding the tetrapeptide on the (110) lattice reflections. The limit of detection the DCNCs-based optical sensor was below 0.005 U/mL, indicating its practicability of application as a sensitive colorimetric sensor for enhanced near-patient testing protease biomarker in treatment of chronic wounds.

In another work, Abdelkader and Kinloch [201] used mechanochemical process in a vertical laboratory attrition mill to produce exfoliated 2D crystals of graphene and transition metal dichalcogenides (TMDs) in a wet media of choline chloride: urea.

In their work, the authors utilized double intercalation of Li^+ and Et_4N^+ ions to achieve exfoliation process and subsequent delamination of the layered crystal within the grinding chamber by shearing. Typically, the resultant material was flakes with 2-5-layers of large diameters of about 5-20 μm and thickness of a thickness between ~0.9-2.5 nm. The authors concluded that the degree of delamination of the layered material gallery was highly dependent on the energy input of the grinding process, which is represented by grinding time and rotational speed. Results showed that the width of the (002) peak was broadened as the speed was increased due to strong attenuation in the π-stacked layers. This indicated the decreasing graphite grain size at 90° to the basal plane. In this study, the choice of choline chloride-urea system was not only because of high dissolution power of about 2.5 wt.% for LiCl to obtain a good concentration of lithium ions but also its biocompatibility, which allows usage of the fabricated 2D ultrathin films in biological applications. Tuntarawongsa's group [202] prepared therapeutic polymers using DES liquid components of menthol and camphor (1:1 ratio) of adequate concentration. The

menthol and camphor components of the eutectic system have been applied as active ingredient in diverse pharmaceuticals. In the resultant DES, Eudragit EPO polymer showed the highest solubility power for up to 40% (w/w) concentration without the individual compounds chemically interacting. Although all the concentrations of the system showed Newtonian behavior, the viscosity depicted an exponential relation with the polymer concentration. Moreover, the type and quantity of polymer slightly affected the pH and surface tension of the system. Summed up, the eutectic mixture of polymers could be beneficial in drug release for pharmaceutical applications [203].

Solvent-assisted deep eutectic syntheses offer an interesting possibility that fits well within green chemistry. For instance, Serrano's group [204] prepared a mixture of octamethylene glycol and lignocaine, a local anesthetic, in appropriate molar ratios to form an low temperature (40°C) eutectic mixture. 2-Hydroxypropane-1,2,3-tricarboxylic acid was easily solubilized in this eutectic mixture and polycondensed with octamethylene glycol at 90°C to obtain lidocaine-loaded polyoctanediol citrate elastomer as a drug eluting material. Belgacem's team [205] extracted nanocellulose (CNCs) using acidic NADES made of choline chloride: oxalic acid dihydrate (1:1 M ratio). With optimized cellulose fiber concentration, temperature and time, the authors evaluated the effects of CNC yield and crystallinity. Experimentally, they found that reacting 2% fiber concentration for 6 hours at boiling point of water, the product yield was about 43.6 %. The extracted CNCs in green solvents could find applications in biocomposite fabrication, biomedical, coatings, hydrogels, and rheological modifiers production. Additional materials such as selenium sulfide nanoparticles [206] have been developed for nanomedicine applications.

4.6. Sustainability assessment of DES-synthesized nanomaterials

Over the last decades, DES have been promoted as green "designer" solvents due to their properties. However, their sustainability is now being scrutinized to understand their toxicological and environmental profiles. Key factors such as biodegradability, ecotoxicity, biotoxicity, feedstock sources, energy consumption, and separation processes need to be considered. Comparing these elements allows for a comprehensive classification of DES sustainability compared to traditional solvents and ionic liquids. Moreover, considering the entire value chain is crucial for assessing DES for various applications [207]. DES offer several sustainable advantages over solvents. *Feedstocks and Recyclability:* Type III DES (quaternary ammonium salts and diverse HBDs like alcohols and amides) and type V DES (low-cost renewable non-ionic molecules) are sustainable due to the recyclability of choline chloride and natural sources for NADES components. Depending on the application, DES can be easily recovered and reused, minimizing waste and reducing overall solvent consumption [208, 209].

Biodegradability: Derived from natural and renewable resources, DES are often biodegradable and environmentally friendly, reducing environmental impact. Most biodegradation studies [208, 210, 211] on DES aqueous solutions with microorganisms have shown about 60% theoretical oxygen demand in the first two weeks [212], validating biodegradation. The choice of individual components affects biodegradability.

Reduced Toxicity: DESs typically exhibit lower toxicity profiles compared to conventional solvents and ionic liquids [208]. In vitro cytotoxicity and toxicity are evaluated using human cell lines and bacteria, showing DESs are safer for human health and the environment [213].

Low Volatility and Energy Efficiency: DES have low volatility, minimizing emissions and health risks for workers [214]. Their low melting points allow for mild reaction conditions, reducing energy requirements and enhancing energy efficiency during nanomaterial synthesis [215].

In summary, while DES offer sustainability benefits, more research is needed on their biodegradability and toxicity to fully understand their environmental impact and ensure safe use in large-scale industrial applications. Particularly, their greenness is not without limitations. Recent review by Chen *et al.* highlighted that DESs, like ionic liquids (ILs), may not always be as environmentally friendly as initially claimed, with concerns about their potential toxicity, biodegradability, stability, and volatility under certain conditions [216]. More research is needed to address these issues and fully understand their environmental impact.

5. Outlook and perspective

The synthesis of nanomaterials has become pivotal in many scientific fields, driven by the demand for materials with unique properties. DESs have emerged as a promising candidate for sustainable nanomaterial synthesis, aligning with the global push towards eco-friendly practices and renewable resources. This review highlights that DESs provide greener and more efficient pathways for nanomaterial production, with key findings including: 1) scalable nanoparticle synthesis with controlled morphology, 2) enhanced CNT and graphene performance, 3) advancement in green polymer science through PDES, and 4) efficient production of tailored nanocrystals and nanofibers for drug delivery and environmental remediation.

However, integrating DESs into nanomaterial synthesis presents challenges, such as: 1) the need for better optimization to control synthesis and material properties, 2) limited exploration of DESs in synthesizing specific nanomaterials like 3D carbon structures, 3) the need for further investigation into catalysis effectiveness in DESs, and 4) higher costs and recyclability challenges compared to conventional organic solvents, requiring more research for sustainable large-scale production.

To address these challenges and unlock the full potential of DESs, future research should focus on: 1) optimizing DES use for better control over nanoparticle properties, 2) exploring novel applications in drug delivery, catalysis, and environmental remediation, and 3) developing sustainable, cost-effective production methods, improving recyclability, and conducting life cycle analyses for long-term scalability.

In conclusion, DESs offer significant opportunities for sustainable nanotechnology, alongside challenges that require innovative solutions. These challenges can serve as catalysts for further research and innovation with exciting prospects, beckoning researchers and practitioners to explore novel pathways, refine methodologies, and pave the way for a sustainable and transformative future in the synthesis of nanomaterials. DESs stand as one of the key drivers in advancing the field of nanomaterials towards a greener and more efficient landscape.

Declaration of competing interest

The authors declare no competing financial interests or personal relationships that could have influenced the work reported in this paper.

Acknowledgements

This Research is supported by the RIE2025 MTC Individual Research Grants (M22K2c0085), administered by the Agency of Science, Technology and Research (A*STAR), Singapore. This work was also supported by the National Medical Research Council (NMRC), Singapore, under its Clinician Scientist-Individual Research Grant (MOH-001357-00).

References

[1] N. Baig, I. Kammakakam, W. Falath, Nanomaterials: a review of synthesis methods, properties, recent progress, and challenges, Materials Advances 2(6) (2021) 1821-1871. https://doi.org/10.1039/D0MA00807A.

[2] C.M. Vineeth Kumar, V. Karthick, V.G. Kumar, D. Inbakandan, E.R. Rene, K.S.U. Suganya, A. Embrandiri, T.S. Dhas, M. Ravi, P. Sowmiya, The impact of engineered nanomaterials on the environment: Release mechanism, toxicity, transformation, and remediation, Environmental Research 212 (2022) 113202. https://doi.org/https://doi.org/10.1016/j.envres.2022.113202.

[3] S.F. Ahmed, M. Mofijur, N. Rafa, A.T. Chowdhury, S. Chowdhury, M. Nahrin, A.B.M.S. Islam, H.C. Ong, Green approaches in synthesising nanomaterials for environmental nanobioremediation: Technological advancements, applications, benefits and challenges, Environmental Research 204 (2022) 111967. https://doi.org/https://doi.org/10.1016/j.envres.2021.111967.

[4] A.P. Abbott, D. Boothby, G. Capper, D.L. Davies, R.K. Rasheed, Deep Eutectic Solvents Formed between Choline Chloride and Carboxylic Acids: Versatile Alternatives to Ionic Liquids, Journal of the American Chemical Society 126(29) (2004) 9142-9147. https://doi.org/10.1021/ja048266j.

[5] T. El Achkar, H. Greige-Gerges, S. Fourmentin, Basics and properties of deep eutectic solvents: a review, Environmental Chemistry Letters 19(4) (2021) 3397-3408. https://doi.org/10.1007/s10311-021-01225-8.

[6] L. Wils, S. Hilali, L. Boudesocque-Delaye, Biomass Valorization Using Natural Deep Eutectic Solvents: What's New in France?, Molecules, 2021.

[7] R. Craveiro, I. Aroso, V. Flammia, T. Carvalho, M.T. Viciosa, M. Dionísio, S. Barreiros, R.L. Reis, A.R.C. Duarte, A. Paiva, Properties and thermal behavior of natural deep eutectic solvents, Journal of Molecular Liquids 215 (2016) 534-540. https://doi.org/https://doi.org/10.1016/j.molliq.2016.01.038.

[8] N.N. Nam, H.D. Do, K.T. Trinh, N.Y. Lee, Design Strategy and Application of Deep Eutectic Solvents for Green Synthesis of Nanomaterials, Nanomaterials, 2023.

[9] M.W. Glasscott, J.E. Dick, Electrodeposition in aqueous nanoreactors, Current Opinion in Electrochemistry 25 (2021) 100637. https://doi.org/https://doi.org/10.1016/j.coelec.2020.09.004.

[10] N.-D. Jaji, M.B.H. Othman, H.L. Lee, M.H. Hussin, D. Hui, One-pot solvothermal synthesis and characterization of highly stable nickel nanoparticles, 10(1) (2021) 318-329. https://doi.org/doi:10.1515/ntrev-2021-0019.

[11] Z. Alhalili, M. Smiri, The Influence of the Calcination Time on Synthesis of Nanomaterials with Small Size, High Crystalline Nature and Photocatalytic Activity in the TiO2 Nanoparticles Calcined at 500 °C, Crystals, 2022.

[12] D. Sundberg, Structured, Composite Nanoparticles from Emulsion Polymerization – Morphological Possibilities, Biomacromolecules 21(11) (2020) 4388-4395. https://doi.org/10.1021/acs.biomac.0c00549.

[13] D. Yu, D. Jiang, Z. Xue, T. Mu, Deep eutectic solvents as green solvents for materials preparation, Green Chemistry 26(13) (2024) 7478-7507. https://doi.org/10.1039/D4GC00136B.

[14] D. Yu, Z. Xue, T. Mu, Deep eutectic solvents as a green toolbox for synthesis, Cell Reports Physical Science 3(4) (2022). https://doi.org/10.1016/j.xcrp.2022.100809.

[15] A. Kalyniukova, J. Holuša, D. Musiolek, J. Sedlakova-Kadukova, J. Płotka-Wasylka, V. Andruch, Application of deep eutectic solvents for separation and determination of bioactive compounds in medicinal plants, Industrial Crops and Products 172 (2021) 114047. https://doi.org/https://doi.org/10.1016/j.indcrop.2021.114047.

[16] J.-H. Liao, P.-C. Wu, Y.-H. Bai, Eutectic mixture of choline chloride/urea as a green solvent in synthesis of a coordination polymer: [Zn(O3PCH2CO2)]·NH4, Inorganic Chemistry Communications 8(4) (2005) 390-392. https://doi.org/https://doi.org/10.1016/j.inoche.2005.01.025.

[17] M.C. Gutiérrez, F. Rubio, F. del Monte, Resorcinol-Formaldehyde Polycondensation in Deep Eutectic Solvents for the Preparation of Carbons and Carbon−Carbon Nanotube Composites, Chemistry of Materials 22(9) (2010) 2711-2719. https://doi.org/10.1021/cm9023502.

[18] C.D. Gu, Y.J. Mai, J.P. Zhou, J.P. Tu, SnO2 NANOCRYSTALLITE: NOVEL SYNTHETIC ROUTE FROM DEEP EUTECTIC SOLVENT AND LITHIUM STORAGE PERFORMANCE, Functional Materials Letters 04(04) (2011) 377-381. https://doi.org/10.1142/S1793604711002251.
[19] J.A. Sirviö, M. Visanko, H. Liimatainen, Deep eutectic solvent system based on choline chloride-urea as a pre-treatment for nanofibrillation of wood cellulose, Green Chemistry 17(6) (2015) 3401-3406. https://doi.org/10.1039/C5GC00398A.
[20] F. Mano, I.M. Aroso, S. Barreiros, J.P. Borges, R.L. Reis, A.R.C. Duarte, A. Paiva, Production of Poly(vinyl alcohol) (PVA) Fibers with Encapsulated Natural Deep Eutectic Solvent (NADES) Using Electrospinning, ACS Sustainable Chemistry & Engineering 3(10) (2015) 2504-2509. https://doi.org/10.1021/acssuschemeng.5b00613.
[21] H. Zhang, X. Qiao, T. Cai, J. Chen, Z. Li, H. Qiu, Preparation and characterization of carbon dot-decorated silica stationary phase in deep eutectic solvents for hydrophilic interaction chromatography, Analytical and Bioanalytical Chemistry 409(9) (2017) 2401-2410. https://doi.org/10.1007/s00216-017-0187-z.
[22] C.-W. Lai, S.-S. Yu, 3D Printable Strain Sensors from Deep Eutectic Solvents and Cellulose Nanocrystals, ACS Applied Materials & Interfaces 12(30) (2020) 34235-34244. https://doi.org/10.1021/acsami.0c11152.
[23] Y. Liu, J.B. Friesen, J.B. McAlpine, D.C. Lankin, S.-N. Chen, G.F. Pauli, Natural deep eutectic solvents: properties, applications, and perspectives, Journal of natural products 81(3) (2018) 679-690.
[24] A.B.B. Junior, G. Pavoski, M.D.C.R. da Silva, W.L. da Silva, D.A. Bertuol, D.C.R. Espinosa, Promising technologies under development for recycling, remanufacturing, and reusing batteries: an introduction, Nano technology for battery recycling, remanufacturing, and reusing, Elsevier2022, pp. 79-103.
[25] S.-L. Cao, W.-M. Gu, W.-D. Ou-Yang, D.-C. Chen, B.-Y. Yang, L.-H. Lai, Y.-D. Wu, Y.-J. Liu, J. Zhu, W.-J. Chen, Preparation, characterization and application of rod-like chitin nanocrystal by using p-toluenesulfonic acid/choline chloride deep eutectic solvent as a hydrolytic media, Carbohydrate polymers 213 (2019) 304-310.
[26] C. Florindo, L.C. Branco, I.M. Marrucho, Quest for green‐solvent design: from hydrophilic to hydrophobic (deep) eutectic solvents, ChemSusChem 12(8) (2019) 1549-1559.
[27] M. Taghizadeh, A. Taghizadeh, V. Vatanpour, M.R. Ganjali, M.R. Saeb, Deep eutectic solvents in membrane science and technology: Fundamental, preparation, application, and future perspective, Separation and Purification Technology 258 (2021) 118015.
[28] A.M. Ramezani, R. Ahmadi, Y. Yamini, Homogeneous liquid-liquid microextraction based on deep eutectic solvents, TrAC Trends in Analytical Chemistry 149 (2022) 116566.
[29] D.O. Abranches, J.A. Coutinho, Type V deep eutectic solvents: Design and applications, Current Opinion in Green and Sustainable Chemistry 35 (2022) 100612.
[30] P. Makoś, G. Boczkaj, Deep eutectic solvents based highly efficient extractive desulfurization of fuels–Eco-friendly approach, Journal of Molecular Liquids 296 (2019) 111916.
[31] C.M. Brett, Deep eutectic solvents and applications in electrochemical sensing, Current Opinion in Electrochemistry 10 (2018) 143-148.
[32] P. Makoś, A. Fernandes, A. Przyjazny, G. Boczkaj, Sample preparation procedure using extraction and derivatization of carboxylic acids from aqueous samples by means of deep eutectic solvents for gas chromatographic-mass spectrometric analysis, Journal of Chromatography A 1555 (2018) 10-19.
[33] C. Velez, O. Acevedo, Simulation of deep eutectic solvents: Progress to promises, Wiley Interdisciplinary Reviews: Computational Molecular Science 12(4) (2022) e1598.
[34] R. Svigelj, N. Dossi, C. Grazioli, R. Toniolo, Deep eutectic solvents (DESs) and their application in biosensor development, Sensors 21(13) (2021) 4263.
[35] M. Zhang, R. Tian, H. Han, K. Wu, B. Wang, Y. Liu, Y. Zhu, H. Lu, B. Liang, Preparation strategy and stability of deep eutectic solvents: a case study based on choline chloride-carboxylic acid, Journal of Cleaner Production 345 (2022) 131028.

[36] C.V. Pereira, J.M. Silva, L. Rodrigues, R.L. Reis, A. Paiva, A.R.C. Duarte, A. Matias, Unveil the anticancer potential of limomene based therapeutic deep eutectic solvents, Scientific reports 9(1) (2019) 14926.
[37] M.S. Rahman, R. Roy, B. Jadhav, M.N. Hossain, M.A. Halim, D.E. Raynie, Formulation, structure, and applications of therapeutic and amino acid-based deep eutectic solvents: An overview, Journal of Molecular Liquids 321 (2021) 114745.
[38] M.M. Abdelquader, S. Li, G.P. Andrews, D.S. Jones, Therapeutic Deep Eutectic Solvents: A Comprehensive Review of Their Thermodynamics, Microstructure and Drug Delivery Applications, European Journal of Pharmaceutics and Biopharmaceutics (2023).
[39] H. Vanda, Y. Dai, E.G. Wilson, R. Verpoorte, Y.H. Choi, Green solvents from ionic liquids and deep eutectic solvents to natural deep eutectic solvents, Comptes Rendus Chimie 21(6) (2018) 628-638.
[40] Y.H. Choi, J. van Spronsen, Y. Dai, M. Verberne, F. Hollmann, I.W. Arends, G.-J. Witkamp, R. Verpoorte, Are natural deep eutectic solvents the missing link in understanding cellular metabolism and physiology?, Plant physiology 156(4) (2011) 1701-1705.
[41] Z. Yang, Natural deep eutectic solvents and their applications in biotechnology, Application of ionic liquids in biotechnology (2019) 31-59.
[42] C.G. González, N.R. Mustafa, E.G. Wilson, R. Verpoorte, Y.H. Choi, Application of natural deep eutectic solvents for the "green" extraction of vanillin from vanilla pods, Flavour and Fragrance Journal 33(1) (2018) 91-96.
[43] A. Mišan, J. Nađpal, A. Stupar, M. Pojić, A. Mandić, R. Verpoorte, Y.H. Choi, The perspectives of natural deep eutectic solvents in agri-food sector, Critical reviews in food science and nutrition 60(15) (2020) 2564-2592.
[44] R. Shi, D. Yu, F. Zhou, J. Yu, T. Mu, An emerging deep eutectic solvent based on halogen-bonds, Chemical Communications 58(29) (2022) 4607-4610. https://doi.org/10.1039/D2CC00528J.
[45] D. Yu, H. Mou, H. Fu, X. Lan, Y. Wang, T. Mu, "Inverted" Deep Eutectic Solvents Based on Host-Guest Interactions, Chemistry – An Asian Journal 14(23) (2019) 4183-4188. https://doi.org/https://doi.org/10.1002/asia.201901365.
[46] D. Yu, T. Mu, Strategy To Form Eutectic Molecular Liquids Based on Noncovalent Interactions, J Phys Chem B 123(23) (2019) 4958-4966. https://doi.org/10.1021/acs.jpcb.9b02891.
[47] A. Isci, M. Kaltschmitt, Recovery and recycling of deep eutectic solvents in biomass conversions: A review, Biomass Conversion and Biorefinery (2021) 1-30.
[48] R.J. Isaifan, A. Amhamed, Review on carbon dioxide absorption by choline chloride/urea deep eutectic solvents, Adv. Chem 2018 (2018) 1-6.
[49] K.A. Omar, R. Sadeghi, Physicochemical properties of deep eutectic solvents: A review, Journal of Molecular Liquids 360 (2022) 119524.
[50] M. Jablonsky, A. Skulcova, A. Haz, J. Sima, V. Majová, Long-term isothermal stability of deep eutectic solvents, BioResources 13(4) (2018) 7545-7559.
[51] I. Cichowska-Kopczyńska, B. Nowosielski, D. Warmińska, Deep Eutectic Solvents: Properties and Applications in CO2 Separation, Molecules, 2023.
[52] R.K. Ibrahim, M. Hayyan, M.A. AlSaadi, S. Ibrahim, A. Hayyan, M.A. Hashim, Physical properties of ethylene glycol-based deep eutectic solvents, Journal of Molecular Liquids 276 (2019) 794-800.
[53] Z. Naseem, R.A. Shehzad, A. Ihsan, J. Iqbal, M. Zahid, A. Pervaiz, G. Sarwari, Theoretical investigation of supramolecular hydrogen-bonded choline chloride-based deep eutectic solvents using density functional theory, Chemical Physics Letters 769 (2021) 138427.
[54] M. Zhang, X. Zhang, Y. Liu, K. Wu, Y. Zhu, H. Lu, B. Liang, Insights into the relationships between physicochemical properties, solvent performance, and applications of deep eutectic solvents, Environmental Science and Pollution Research 28(27) (2021) 35537-35563.
[55] G. Gygli, X. Xu, J. Pleiss, Meta-analysis of viscosity of aqueous deep eutectic solvents and their components, Scientific reports 10(1) (2020) 21395.

[56] C. Florindo, M.M. Oliveira, L.C. Branco, I.M. Marrucho, Carbohydrates-based deep eutectic solvents: Thermophysical properties and rice straw dissolution, Journal of Molecular Liquids 247 (2017) 441-447. https://doi.org/https://doi.org/10.1016/j.molliq.2017.09.026.
[57] Z. Maugeri, P. Domínguez de María, Novel choline-chloride-based deep-eutectic-solvents with renewable hydrogen bond donors: levulinic acid and sugar-based polyols, RSC Advances 2(2) (2012) 421-425. https://doi.org/10.1039/C1RA00630D.
[58] D. Shi, F. Zhou, W. Mu, C. Ling, T. Mu, G. Yu, R. Li, Deep insights into the viscosity of deep eutectic solvents by an XGBoost-based model plus SHapley Additive exPlanation, Physical Chemistry Chemical Physics 24(42) (2022) 26029-26036. https://doi.org/10.1039/D2CP03423A.
[59] R.J. Nunes, B. Saramago, I.M. Marrucho, Surface tension of dl-menthol: octanoic acid eutectic mixtures, Journal of Chemical & Engineering Data 64(11) (2019) 4915-4923.
[60] T. El Achkar, H. Greige-Gerges, S. Fourmentin, Basics and properties of deep eutectic solvents: a review, Environmental chemistry letters 19 (2021) 3397-3408.
[61] M.H. Shafie, R. Yusof, C.-Y. Gan, Synthesis of citric acid monohydrate-choline chloride based deep eutectic solvents (DES) and characterization of their physicochemical properties, Journal of Molecular Liquids 288 (2019) 111081.
[62] Y. Zhou, W. Wu, N. Zhang, O.P. Soladoye, Y. Zhang, Y. Fu, Deep eutectic solvents as new media for green extraction of food proteins: Opportunity and challenges, Food Research International 161 (2022) 111842.
[63] T. Lemaoui, A. Boublia, A.S. Darwish, M. Alam, S. Park, B.-H. Jeon, F. Banat, Y. Benguerba, I.M. AlNashef, Predicting the surface tension of deep eutectic solvents using artificial neural networks, ACS omega 7(36) (2022) 32194-32207.
[64] Y. Chen, W. Chen, L. Fu, Y. Yang, Y. Wang, X. Hu, F. Wang, T. Mu, Surface tension of 50 deep eutectic solvents: effect of hydrogen-bonding donors, hydrogen-bonding acceptors, other solvents, and temperature, Industrial & Engineering Chemistry Research 58(28) (2019) 12741-12750.
[65] Z.X.U.E.J.W.J.J.X.Z.T.M.U. Wenjun Chen, Investigation on the Thermal Stability of Deep Eutectic Solvents, Acta Physico-Chimica Sinica 34(8) (2018) 904-911.
[66] Q. Li, J. Jiang, G. Li, W. Zhao, X. Zhao, T. Mu, The electrochemical stability of ionic liquids and deep eutectic solvents, Science China Chemistry 59(5) (2016) 571-577. https://doi.org/10.1007/s11426-016-5566-3.
[67] Y. Wang, W. Chen, Q. Zhao, G. Jin, Z. Xue, Y. Wang, T. Mu, Ionicity of deep eutectic solvents by Walden plot and pulsed field gradient nuclear magnetic resonance (PFG-NMR), Physical Chemistry Chemical Physics 22(44) (2020) 25760-25768. https://doi.org/10.1039/D0CP01431A.
[68] A. Azzouz, M. Hayyan, Potential applications of deep eutectic solvents in nanotechnology: Part II, Chemical Engineering Journal (2023) 143563.
[69] D. Lapeña, L. Lomba, M. Artal, C. Lafuente, B. Giner, The NADES glyceline as a potential Green Solvent: A comprehensive study of its thermophysical properties and effect of water inclusion, The Journal of Chemical Thermodynamics 128 (2019) 164-172.
[70] P. Makoś-Chełstowska, M. Kaykhaii, J. Płotka-Wasylka, M. de la Guardia, Magnetic deep eutectic solvents–Fundamentals and applications, Journal of Molecular Liquids 365 (2022) 120158.
[71] M.Q. Farooq, N.M. Abbasi, J.L. Anderson, Deep eutectic solvents in separations: Methods of preparation, polarity, and applications in extractions and capillary electrochromatography, Journal of Chromatography a 1633 (2020) 461613.
[72] C. Florindo, A. McIntosh, T. Welton, L. Branco, I. Marrucho, A closer look into deep eutectic solvents: exploring intermolecular interactions using solvatochromic probes, Physical Chemistry Chemical Physics 20(1) (2018) 206-213.
[73] S.M. Taklimi, A. Divsalar, B. Ghalandari, X. Ding, M.L. Di Gioia, K.A. Omar, A.A. Saboury, Effects of deep eutectic solvents on the activity and stability of enzymes, Journal of Molecular Liquids 377 (2023) 121562.

[74] A.P. Abbott, R.C. Harris, K.S. Ryder, C. D'Agostino, L.F. Gladden, M.D. Mantle, Glycerol eutectics as sustainable solvent systems, Green Chemistry 13(1) (2011) 82-90. https://doi.org/10.1039/C0GC00395F.
[75] X. Shi, Z. Wang, S. Liu, Q. Xia, Y. Liu, W. Chen, H. Yu, K. Zhang, Scalable production of carboxylated cellulose nanofibres using a green and recyclable solvent, Nature Sustainability 7(3) (2024) 315-325. https://doi.org/10.1038/s41893-024-01267-0.
[76] A.A. Quintana, A.M. Sztapka, V.d.C. Santos Ebinuma, C. Agatemor, Enabling sustainable chemistry with ionic liquids and deep eutectic solvents: a fad or the future?, Angewandte Chemie 134(37) (2022) e202205609.
[77] M. Hayyan, M.A. Hashim, A. Hayyan, M.A. Al-Saadi, I.M. AlNashef, M.E. Mirghani, O.K. Saheed, Are deep eutectic solvents benign or toxic?, Chemosphere 90(7) (2013) 2193-2195.
[78] M. Marchel, H. Cieśliński, G. Boczkaj, Deep eutectic solvents microbial toxicity: Current state of art and critical evaluation of testing methods, Journal of Hazardous Materials 425 (2022) 127963.
[79] L. Lomba, M.P. Ribate, E. Sangüesa, J. Concha, M.P. Garralaga, D. Errazquin, C.B. García, B. Giner, Deep eutectic solvents: Are they safe?, Applied Sciences 11(21) (2021) 10061.
[80] Y. Li, J. Luo, S. Shan, Y. Cao, High toxicity of amino acid-based deep eutectic solvents, Journal of Molecular Liquids 370 (2023) 121044.
[81] J. Torregrosa-Crespo, X. Marset, G. Guillena, D.J. Ramon, R.M. Martínez-Espinosa, New guidelines for testing "Deep eutectic solvents" toxicity and their effects on the environment and living beings, Science of the Total Environment 704 (2020) 135382.
[82] A. Prabhune, R. Dey, Green and sustainable solvents of the future: Deep eutectic solvents, Journal of Molecular Liquids 379 (2023) 121676.
[83] Z. Yang, Toxicity and biodegradability of deep eutectic solvents and natural deep eutectic solvents, Deep eutectic solvents: synthesis, properties, and applications (2019) 43-60.
[84] A. Azzouz, M. Hayyan, Are deep eutectic solvents biodegradable?, Process Safety and Environmental Protection (2023).
[85] S. Datta, J. Mahin, E. Liberti, I. Manasi, K.J. Edler, L. Torrente-Murciano, Role of the Deep Eutectic Solvent Reline in the Synthesis of Gold Nanoparticles, ACS Sustainable Chemistry & Engineering 11(28) (2023) 10242-10251. https://doi.org/10.1021/acssuschemeng.2c07337.
[86] L. Adhikari, N.E. Larm, G.A. Baker, Batch and Flow Nanomanufacturing of Large Quantities of Colloidal Silver and Gold Nanocrystals Using Deep Eutectic Solvents, ACS Sustainable Chemistry & Engineering 8(39) (2020) 14679-14689. https://doi.org/10.1021/acssuschemeng.0c04244.
[87] H.-G. Liao, Y.-X. Jiang, Z.-Y. Zhou, S.-P. Chen, S.-G. Sun, Shape-Controlled Synthesis of Gold Nanoparticles in Deep Eutectic Solvents for Studies of Structure–Functionality Relationships in Electrocatalysis, Angewandte Chemie International Edition 47(47) (2008) 9100-9103. https://doi.org/https://doi.org/10.1002/anie.200803202.
[88] K. Rong, L. Huang, H. Zhang, J. Zhai, Y. Fang, S. Dong, Electrochemical fabrication of nanoporous gold electrodes in a deep eutectic solvent for electrochemical detections, Chemical Communications 54(64) (2018) 8853-8856. https://doi.org/10.1039/C8CC04454F.
[89] L. Adhikari, N.E. Larm, N. Bhawawet, G.A. Baker, Rapid Microwave-Assisted Synthesis of Silver Nanoparticles in a Halide-Free Deep Eutectic Solvent, ACS Sustainable Chemistry & Engineering 6(5) (2018) 5725-5731. https://doi.org/10.1021/acssuschemeng.8b00050.
[90] F. Chen, S. Xie, J. Zhang, R. Liu, Synthesis of spherical Fe3O4 magnetic nanoparticles by co-precipitation in choline chloride/urea deep eutectic solvent, Materials Letters 112 (2013) 177-179. https://doi.org/https://doi.org/10.1016/j.matlet.2013.09.022.
[91] H. Chen, W. Jiang, N. Zhao, X. Zhang, X. Ma, H. Jia, Y. Zhuang, M. Guan, A novel method for synthesizing one or two-dimensional metal oxide (hydroxide) nanomaterials using deep eutectic solvents, New Journal of Chemistry 47(16) (2023) 7903-7909. https://doi.org/10.1039/D3NJ01187A.
[92] J.-Y. Dong, C.-H. Lin, Y.-J. Hsu, S.-Y. Lu, D.S.-H. Wong, Single-crystalline mesoporous ZnO nanosheets prepared with a green antisolvent method exhibiting excellent photocatalytic efficiencies, CrystEngComm 14(14) (2012) 4732-4737. https://doi.org/10.1039/C2CE06739K.

[93] Y. Liu, S. Kang, K. Li, J. Chen, B. Bae, I. Hwang, E.-Y. Ahn, Y. Park, K.-H. Chun, J. Lee, Ecofriendly and enhanced biogenic synthesis of silver nanoparticles using deep eutectic solvent-based green tea extracts, Journal of Cleaner Production 379 (2022) 134655. https://doi.org/https://doi.org/10.1016/j.jclepro.2022.134655.
[94] S. K, I. D, Silver Nanoparticles: Synthesis in Newly Formed Ternary Deep Eutectic Solvent Media, Characterization and their Antifungal Activity, Current Nanomaterials 8(3) (2023) 280-290. https://doi.org/http://dx.doi.org/10.2174/2405461507666220817155944.
[95] G.P. Longatto, K.K.L. Augusto, P.C. Gomes Júnior, R.O. Gonçalves, J.C.O. Almeida, E.T.G. Cavalheiro, O. Fatibello Filho, Development of electrochemical sensors with metallic nanoparticles synthesized in deep eutectic solvents, Reunião Anual da Sociedade Brasileira de Química - RASBQ, 2023.
[96] O.S. Hammond, K.J. Edler, D.T. Bowron, L. Torrente-Murciano, Deep eutectic-solvothermal synthesis of nanostructured ceria, Nature Communications 8(1) (2017) 14150. https://doi.org/10.1038/ncomms14150.
[97] J. Iqbal, N.S. Shah, M. Sayed, N. Muhammad, S.-u. Rehman, J.A. Khan, Z.U. Haq Khan, F.M. Howari, Y. Nazzal, C. Xavier, S. Arshad, A. Hussein, K. Polychronopoulou, Deep eutectic solvent-mediated synthesis of ceria nanoparticles with the enhanced yield for photocatalytic degradation of flumequine under UV-C, Journal of Water Process Engineering 33 (2020) 101012. https://doi.org/https://doi.org/10.1016/j.jwpe.2019.101012.
[98] O.S. Hammond, R.S. Atri, D.T. Bowron, L. de Campo, S. Diaz-Moreno, L.L. Keenan, J. Doutch, S. Eslava, K.J. Edler, Structural evolution of iron forming iron oxide in a deep eutectic-solvothermal reaction, Nanoscale 13(3) (2021) 1723-1737. https://doi.org/10.1039/D0NR08372K.
[99] X. Lai, G. Luo, Synthesis of mesoporous α-MnO2 in manganese(II)-based deep eutectic solvent and their application in the absorption of Congo red, Separation Science and Technology 54(8) (2019) 1269-1277. https://doi.org/10.1080/01496395.2018.1535605.
[100] X. Ge, C.D. Gu, X.L. Wang, J.P. Tu, Spinel type CoFe oxide porous nanosheets as magnetic adsorbents with fast removal ability and facile separation, Journal of Colloid and Interface Science 454 (2015) 134-143. https://doi.org/https://doi.org/10.1016/j.jcis.2015.05.013.
[101] I.A. Lawal, T.H. Dolla, K. Pruessner, P. Ndungu, Synthesis and characterization of deep eutectic solvent functionalized CNT/ZnCo2O4 nanostructure: Kinetics, isotherm and regenerative studies on Eosin Y adsorption, Journal of Environmental Chemical Engineering 7(1) (2019) 102877. https://doi.org/https://doi.org/10.1016/j.jece.2018.102877.
[102] Q. Shan, Q. Ding, W. Wu, Preparation of Antioxidative MXene by Deep Eutectic Solvent-Assisted Electrochemical Ultrasonic Composite Exfoliation and Its Application in Flexible Solid-State Supercapacitors, Industrial & Engineering Chemistry Research 62(24) (2023) 9492-9502. https://doi.org/10.1021/acs.iecr.3c00989.
[103] S. Gong, F. Zhao, Y. Zhang, H. Xu, M. Li, J. Qi, H. Wang, Z. Wang, Y. Hu, X. Fan, W. Peng, C. Li, J. Liu, Few-layered Ti3C2Tx MXene synthesized via water-free etching toward high-performance supercapacitors, Journal of Colloid and Interface Science 632 (2023) 216-222. https://doi.org/https://doi.org/10.1016/j.jcis.2022.11.063.
[104] N. Wang, A.-Q. Zheng, X. Liu, J.-J. Chen, T. Yang, M.-L. Chen, J.-H. Wang, Deep Eutectic Solvent-Assisted Preparation of Nitrogen/Chloride-Doped Carbon Dots for Intracellular Biological Sensing and Live Cell Imaging, ACS Applied Materials & Interfaces 10(9) (2018) 7901-7909. https://doi.org/10.1021/acsami.8b00947.
[105] Z. Gao, X. Li, L. Shi, Y. Yang, Deep eutectic solvents-derived carbon dots for detection of mercury (II), photocatalytic antifungal activity and fluorescent labeling for C. albicans, Spectrochim Acta A Mol Biomol Spectrosc 220 (2019) 117080. https://doi.org/10.1016/j.saa.2019.04.072.
[106] Q. Yin, M. Wang, D. Fang, Y. Zhu, L. Yang, Novel N,Cl-doped deep eutectic solvents-based carbon dots as a selective fluorescent probe for determination of morphine in food, RSC Advances 11(27) (2021) 16805-16813. https://doi.org/10.1039/D1RA00886B.

[107] R. Tabaraki, F. Nazari, Comparison of Carbon Dots Prepared in Deep Eutectic Solvent and Water/Deep Eutectic Solvent: Study of Fluorescent Detection of Fe3+ and Cetirizine and their Photocatalytic Antibacterial Activity, Journal of Fluorescence 32(2) (2022) 549-558. https://doi.org/10.1007/s10895-021-02875-1.
[108] N. Zhao, J. Song, L. Zhao, Metallic deep eutectic solvents-assisted synthesis of Cu, Cl-doped carbon dots as oxidase-like and peroxidase-like nanozyme for colorimetric assay of hydroquinone and H2O2, Colloids and Surfaces A: Physicochemical and Engineering Aspects 648 (2022) 129390. https://doi.org/https://doi.org/10.1016/j.colsurfa.2022.129390.
[109] H. Ren, Y. Liu, R. Zhang, Y. Zheng, T. Zhao, J. Han, C. Chen, E. Duan, Near-infrared carbon quantum dots from PEG-based deep eutectic solvents for high-accuracy quantitative analysis of naphthenic acids in wastewater, Journal of Environmental Chemical Engineering 11(3) (2023) 109988. https://doi.org/https://doi.org/10.1016/j.jece.2023.109988.
[110] Z. Guo, H.-Y. Zheng, Z.-Y. Huang, Y.-Z. Liu, Y.-H. Liu, Y. Chen, J. Gao, Y. Hu, C. Huang, Solvothermal synthesis of bifunctional carbon dots for tartrazine and Fe(III) detection from chamomile residue by ternary DES pretreatment, Food Chemistry 426 (2023) 136604. https://doi.org/https://doi.org/10.1016/j.foodchem.2023.136604.
[111] M.K. AlOmar, M.A. Alsaadi, M. Hayyan, S. Akib, M.A. Hashim, Functionalization of CNTs surface with phosphonuim based deep eutectic solvents for arsenic removal from water, Applied Surface Science 389 (2016) 216-226. https://doi.org/https://doi.org/10.1016/j.apsusc.2016.07.079.
[112] M.K. AlOmar, M.A. Alsaadi, M. Hayyan, S. Akib, M. Ibrahim, M.A. Hashim, Allyl triphenyl phosphonium bromide based DES-functionalized carbon nanotubes for the removal of mercury from water, Chemosphere 167 (2017) 44-52. https://doi.org/https://doi.org/10.1016/j.chemosphere.2016.09.133.
[113] M. Khalid, M. Al-Saadi, M. Aljumaily, S. Akib, T. Jassam, M. Hashim, N,N-diethylethanolammonium chloride based DES-functionalized carbon nanotubes for arsenic removal from aqueous solution, Desalination and water treatment 74 (2017) 163-173. https://doi.org/10.5004/dwt.2017.20562.
[114] R. Ibrahim, M. Al-Saadi, M. Khalid, S. Ibrahim, Adsorption of 2,4-dichlorophenol from water using deep eutectic solvents-functionalized carbon nanotubes, DESALINATION AND WATER TREATMENT 116 (2018) 214-231. https://doi.org/10.5004/dwt.2018.22485.
[115] R.K. Ibrahim, S.S. Fiyadh, M.A. AlSaadi, L.S. Hin, N.S. Mohd, S. Ibrahim, H.A. Afan, C.M. Fai, A.N. Ahmed, A. Elshafie, Feedforward Artificial Neural Network-Based Model for Predicting the Removal of Phenolic Compounds from Water by Using Deep Eutectic Solvent-Functionalized CNTs, Molecules, 2020.
[116] L.-H. Ye, J. Yang, B. Wang, Q.-Y. Wang, F. Liu, L.-J. Du, J. Cao, A novel non-covalent functionalized multi-walled carbon nanotubes for the microextraction of bromophenols in kelp and seaweed, Microchemical Journal 151 (2019) 104205. https://doi.org/https://doi.org/10.1016/j.microc.2019.104205.
[117] Q. Zaib, I. Adeyemi, D.M. Warsinger, I.M. AlNashef, Deep Eutectic Solvent Assisted Dispersion of Carbon Nanotubes in Water, Frontiers in Chemistry 8 (2020). https://doi.org/10.3389/fchem.2020.00808.
[118] X. Wang, G. Li, K.H. Row, Graphene and Graphene Oxide Modified by Deep Eutectic Solvents and Ionic Liquids Supported on Silica as Adsorbents for Solid-Phase Extraction, Bulletin of the Korean Chemical Society 38(2) (2017) 251-257. https://doi.org/https://doi.org/10.1002/bkcs.11074.
[119] N. Lamei, M. Ezoddin, M.S. Ardestani, K. Abdi, Dispersion of magnetic graphene oxide nanoparticles coated with a deep eutectic solvent using ultrasound assistance for preconcentration of methadone in biological and water samples followed by GC–FID and GC–MS, Analytical and Bioanalytical Chemistry 409(26) (2017) 6113-6121. https://doi.org/10.1007/s00216-017-0547-8.
[120] H. Lin, K. Gong, W. Ying, D. Chen, J. Zhang, Y. Yan, X. Peng, CO2-Philic Separation Membrane: Deep Eutectic Solvent Filled Graphene Oxide Nanoslits, Small 15(49) (2019) 1904145. https://doi.org/https://doi.org/10.1002/smll.201904145.

[121] Y.-F. Shen, X. Zhang, C.-E. Mo, Y.-P. Huang, Z.-S. Liu, Preparation of graphene oxide incorporated monolithic chip based on deep eutectic solvents for solid phase extraction, Analytica Chimica Acta 1096 (2020) 184-192. https://doi.org/https://doi.org/10.1016/j.aca.2019.10.041.
[122] Q. Zhang, K.D.O. Vigier, S. Royer, F. Jerome, Deep eutectic solvents: syntheses, properties and applications., Chem. Soc. Rev. 41 (2012) 7108–7146.
[123] P.M.V. Fernandes, J.M. Campiña, N.M. Pereira, C.M. Pereira, F. Silva, Biodegradable deep-eutectic mixtures as electrolytes for the electrochemical synthesis of conducting polymers, Journal of Applied Electrochemistry 42(12) (2012) 997-1003. https://doi.org/10.1007/s10800-012-0474-5.
[124] L. Liu, S.-M. Wang, W.-L. Chen, Y. Lu, Y.-G. Li, E.-B. Wang, A high nuclear lanthanide-containing polyoxometalate aggregate synthesized in choline chloride/urea eutectic mixture, Inorganic Chemistry Communications 23 (2012) 14-16.
[125] F. Lionetto, A. Timo, M. Frigione, Curing kinetics of epoxy-deep eutectic solvent mixtures, Thermochimica Acta 612 (2015) 70-78.
[126] A.R.S. Santha Kumar, N.K. Singha, RAFT polymerization of 2 ‐ hydroxyethyl methacrylate in a deep eutectic solvent, Journal of Polymer Science Part A: Polymer Chemistry 57(23) (2019) 2281-2286. https://doi.org/10.1002/pola.29527.
[127] S. Bednarz, K. Półćwiartek, J. Wityk, B. Strachota, J. Kredatusová, H. Beneš, A. Wesołowska-Piętak, G. Kowalski, Polymerization-crosslinking of renewable itaconic acid in water and in deep eutectic solvents, European Polymer Journal 95 (2017) 241-254. https://doi.org/10.1016/j.eurpolymj.2017.08.020.
[128] J. Ruiz-Olles, P. Slavik, N.K. Whitelaw, D.K. Smith, Self-Assembled Gels Formed in Deep Eutectic Solvents: Supramolecular Eutectogels with High Ionic Conductivity, Angew Chem Int Ed Engl 58(13) (2019) 4173-4178. https://doi.org/10.1002/anie.201810600.
[129] C. Gu, Y. Peng, J. Li, H. Wang, X.Q. Xie, X. Cao, C.S. Liu, Supramolecular G4 Eutectogels of Guanosine with Solvent-Induced Chiral Inversion and Excellent Electrochromic Activity, Angew Chem Int Ed Engl 59(42) (2020) 18768-18773. https://doi.org/10.1002/anie.202009332.
[130] J.D. Mota-Morales, M.C. Gutierrez, I.C. Sanchez, G. Luna-Barcenas, F. del Monte, Frontal polymerizations carried out in Deep-Eutectic mixtures providing both the monomers and the polymerization medium, Chem Commun (Camb) 47(18) (2011) 5328-30. https://doi.org/10.1039/c1cc10391a.
[131] J.D. Mota-Morales, M.C. Gutiérrez, M.L. Ferrer, R. Jiménez, P. Santiago, I.C. Sanchez, M. Terrones, F. Del Monte, G. Luna-Bárcenas, Synthesis of macroporous poly(acrylic acid)–carbon nanotube composites by frontal polymerization in deep-eutectic solvents, Journal of Materials Chemistry A 1(12) (2013). https://doi.org/10.1039/c3ta01020a.
[132] M. Wang, R. Li, G. Chen, S. Zhou, X. Feng, Y. Chen, M. He, D. Liu, T. Song, H. Qi, Highly Stretchable, Transparent, and Conductive Wood Fabricated by in Situ Photopolymerization with Polymerizable Deep Eutectic Solvents, ACS Appl Mater Interfaces 11(15) (2019) 14313-14321. https://doi.org/10.1021/acsami.9b00728.
[133] M. Wang, R. Li, X. Feng, C. Dang, F. Dai, X. Yin, M. He, D. Liu, H. Qi, Cellulose Nanofiber-Reinforced Ionic Conductors for Multifunctional Sensors and Devices, ACS Appl Mater Interfaces 12(24) (2020) 27545-27554. https://doi.org/10.1021/acsami.0c04907.
[134] R.a. Li, T. Fan, G. Chen, H. Xie, B. Su, M. He, Highly transparent, self-healing conductive elastomers enabled by synergistic hydrogen bonding interactions, Chemical Engineering Journal 393 (2020). https://doi.org/10.1016/j.cej.2020.124685.
[135] M. Castillo-Santillan, J.R. Torres-Lubian, A. Martínez-Richa, S.T. Huerta-Marcial, M.C. Gutierrez, K. Loos, M.G. Peréz-García, J.D. Mota-Morales, From polymer blends to a block copolymer: Ring-opening polymerization of L-lactide/ε-caprolactone eutectic system, Polymer 262 (2022). https://doi.org/10.1016/j.polymer.2022.125432.
[136] W.-L. Lim, A.A.N. Gunny, F.H. Kasim, S.C.B. Gopinath, N.H.I. Kamaludin, D. Arbain, Cellulose nanocrystals from bleached rice straw pulp: acidic deep eutectic solvent versus sulphuric acid hydrolyses, Cellulose 28(10) (2021) 6183-6199. https://doi.org/10.1007/s10570-021-03914-7.

[137] X. Yang, H. Xie, H. Du, X. Zhang, Z. Zou, Y. Zou, W. Liu, H. Lan, X. Zhang, C. Si, Facile Extraction of Thermally Stable and Dispersible Cellulose Nanocrystals with High Yield via a Green and Recyclable FeCl3-Catalyzed Deep Eutectic Solvent System, ACS Sustainable Chemistry & Engineering 7(7) (2019) 7200-7208. https://doi.org/10.1021/acssuschemeng.9b00209.
[138] O. Laitinen, J. Ojala, J.A. Sirviö, H. Liimatainen, Sustainable stabilization of oil in water emulsions by cellulose nanocrystals synthesized from deep eutectic solvents, Cellulose 24(4) (2017) 1679-1689. https://doi.org/10.1007/s10570-017-1226-9.
[139] Q. Fan, C. Jiang, W. Wang, L. Bai, H. Chen, H. Yang, D. Wei, L. Yang, Eco-friendly extraction of cellulose nanocrystals from grape pomace and construction of self-healing nanocomposite hydrogels, Cellulose 27(5) (2020) 2541-2553. https://doi.org/10.1007/s10570-020-02977-2.
[140] M. Wu, K. Liao, C. Liu, G. Yu, M. Rahmaninia, H. Li, B. Li, Integrated and sustainable preparation of functional nanocellulose via formic acid/choline chloride solvents pretreatment, Cellulose 28 (2021). https://doi.org/10.1007/s10570-021-04157-2.
[141] Y. Ma, Q. Xia, Y. Liu, W. Chen, S. Liu, Q. Wang, Y. Liu, J. Li, H. Yu, Production of Nanocellulose Using Hydrated Deep Eutectic Solvent Combined with Ultrasonic Treatment, ACS Omega 4(5) (2019) 8539-8547. https://doi.org/10.1021/acsomega.9b00519.
[142] H. Zhang, Y. Wu, J. Zhang, Z. Wu, X. Zhan, Separation cellulose nanocrystals from microcrystalline cellulose using hydrated deep eutectic solvent and high shear force, Industrial Crops and Products 189 (2022) 115781. https://doi.org/https://doi.org/10.1016/j.indcrop.2022.115781.
[143] M.A. Smirnov, M.P. Sokolova, D.A. Tolmachev, V.K. Vorobiov, I.A. Kasatkin, N.N. Smirnov, A.V. Klaving, N.V. Bobrova, N.V. Lukasheva, A.V. Yakimansky, Green method for preparation of cellulose nanocrystals using deep eutectic solvent, Cellulose 27(8) (2020) 4305-4317. https://doi.org/10.1007/s10570-020-03100-1.
[144] S. Liu, Q. Zhang, S. Gou, L. Zhang, Z. Wang, Esterification of cellulose using carboxylic acid-based deep eutectic solvents to produce high-yield cellulose nanofibers, Carbohydrate Polymers 251 (2021) 117018. https://doi.org/https://doi.org/10.1016/j.carbpol.2020.117018.
[145] H. Zhang, Y. Shi, M. Li, J. Chen, Y. Xin, L. Zhang, Z. Gu, J. Liu, R. Liu, Extraction of lignin from corncob residue via a deep eutectic solvent for the preparation of nanoparticles by self-assembly, Chemical Engineering Science 256 (2022) 117694. https://doi.org/https://doi.org/10.1016/j.ces.2022.117694.
[146] S. Hong, Y. Yuan, Q. Yang, L. Chen, J. Deng, W. Chen, H. Lian, J.D. Mota-Morales, H. Liimatainen, Choline chloride-zinc chloride deep eutectic solvent mediated preparation of partial O-acetylation of chitin nanocrystal in one step reaction, Carbohydrate Polymers 220 (2019) 211-218. https://doi.org/https://doi.org/10.1016/j.carbpol.2019.05.075.
[147] Z. Ling, J.V. Edwards, Z. Guo, N.T. Prevost, S. Nam, Q. Wu, A.D. French, F. Xu, Structural variations of cotton cellulose nanocrystals from deep eutectic solvent treatment: micro and nano scale, Cellulose 26(2) (2019) 861-876. https://doi.org/10.1007/s10570-018-2092-9.
[148] W. Yu, C. Wang, Y. Yi, H. Wang, Y. Yang, L. Zeng, Z. Tan, Direct pretreatment of raw ramie fibers using an acidic deep eutectic solvent to produce cellulose nanofibrils in high purity, Cellulose 28(1) (2021) 175-188. https://doi.org/10.1007/s10570-020-03538-3.
[149] J.A. Sirviö, J. Ukkola, H. Liimatainen, Direct sulfation of cellulose fibers using a reactive deep eutectic solvent to produce highly charged cellulose nanofibers, Cellulose 26 (2019) 2303-2316.
[150] W. Li, Y. Xue, M. He, J. Yan, L.A. Lucia, J. Chen, J. Yu, G. Yang, Facile Preparation and Characteristic Analysis of Sulfated Cellulose Nanofibril via the Pretreatment of Sulfamic Acid-Glycerol Based Deep Eutectic Solvents, Nanomaterials, 2021.
[151] W. Liu, H. Du, K. Liu, H. Liu, H. Xie, C. Si, B. Pang, X. Zhang, Sustainable preparation of cellulose nanofibrils via choline chloride-citric acid deep eutectic solvent pretreatment combined with high-pressure homogenization, Carbohydrate Polymers 267 (2021) 118220. https://doi.org/https://doi.org/10.1016/j.carbpol.2021.118220.
[152] M. Yan, C. Tian, T. Wu, X. Huang, Y. Zhong, P. Yang, L. Zhang, J. Ma, H. Lu, X. Zhou, Insights into structure and properties of cellulose nanofibrils (CNFs) prepared by screw extrusion and deep eutectic

718 solvent permeation, International Journal of Biological Macromolecules 191 (2021) 422-431.
719 https://doi.org/https://doi.org/10.1016/j.ijbiomac.2021.09.105.
720 [153] Z. Wei, D. Wang, Y. Chen, D. Yu, Q. Ding, R. Li, C. Wu, The H-bond evolution of cellulose
721 nanofibrils treated with choline chloride/oxalic acid, Cellulose 29 (2022).
722 https://doi.org/10.1007/s10570-022-04517-6.
723 [154] T. Luo, C. Wang, X. Ji, G. Yang, J. Chen, C.G. Yoo, S. Janaswamy, G. Lyu, Innovative production of
724 lignin nanoparticles using deep eutectic solvents for multifunctional nanocomposites, International
725 Journal of Biological Macromolecules 183 (2021). https://doi.org/10.1016/j.ijbiomac.2021.05.005.
726 [155] X. Yue, T. Suopajärvi, S. Sun, O. Mankinen, A. Mikkelson, H. Huttunen, S. Komulainen, I.
727 Romakkaniemi, J. Ahola, V.-V. Telkki, H. Liimatainen, High-purity lignin fractions and nanospheres rich
728 in phenolic hydroxyl and carboxyl groups isolated with alkaline deep eutectic solvent from wheat
729 straw, Bioresource Technology 360 (2022) 127570.
730 https://doi.org/https://doi.org/10.1016/j.biortech.2022.127570.
731 [156] W.-H. Gong, C. Zhang, J.-W. He, Y.-Y. Gao, Y.-J. Li, M.-Q. Zhu, J.-L. Wen, A synergistic
732 hydrothermal-deep eutectic solvents (DES) pretreatment for acquiring xylooligosaccharides and lignin
733 nanoparticles from Eucommia ulmoides wood, International Journal of Biological Macromolecules 209
734 (2022) 188-197. https://doi.org/https://doi.org/10.1016/j.ijbiomac.2022.04.008.
735 [157] Z. Yan, Z. Wang, Y. Chen, C. Liu, Y. Liu, R. Li, M. Si, Y. Shi, Preparation of lignin nanoparticles via
736 ultra-fast microwave-assisted fractionation of lignocellulose using ternary deep eutectic solvents,
737 Biotechnology and Bioengineering 120(6) (2023) 1557-1568.
738 https://doi.org/https://doi.org/10.1002/bit.28373.
739 [158] D. Tian, F. Shen, J. Hu, M. Huang, L. Zhao, J. He, Q. Li, S. Zhang, F. Shen, Complete conversion of
740 lignocellulosic biomass into three high-value nanomaterials through a versatile integrated technical
741 platform, Chemical Engineering Journal 428 (2022) 131373.
742 https://doi.org/https://doi.org/10.1016/j.cej.2021.131373.
743 [159] Y. Xu, S.-C. Sun, C. Zhang, C.-Y. Ma, J.-L. Wen, T.-Q. Yuan, Complete valorization of bamboo
744 biomass into multifunctional nanomaterials by reactive deep eutectic solvent pretreatment: Towards
745 a waste-free biorefinery, Chemical Engineering Journal 462 (2023) 142213.
746 https://doi.org/https://doi.org/10.1016/j.cej.2023.142213.
747 [160] C.-Y. Ma, X.-P. Peng, S. Sun, J.-L. Wen, T.-Q. Yuan, Short-time deep eutectic solvents
748 pretreatment enhanced production of fermentable sugars and tailored lignin nanoparticles from
749 abaca, International Journal of Biological Macromolecules 192 (2021) 417-425.
750 https://doi.org/https://doi.org/10.1016/j.ijbiomac.2021.09.140.
751 [161] T. Luo, Y. Hao, C. Wang, W. Jiang, X. Ji, G. Yang, J. Chen, S. Janaswamy, G. Lyu, Lignin
752 Nanoparticles and Alginate Gel Beads: Preparation, Characterization and Removal of Methylene Blue,
753 Nanomaterials 12 (2022) 176. https://doi.org/10.3390/nano12010176.
754 [162] C. Mukesh, D. Mondal, M. Sharma, K. Prasad, Choline chloride–thiourea, a deep eutectic solvent
755 for the production of chitin nanofibers, Carbohydrate Polymers 103 (2014) 466-471.
756 https://doi.org/https://doi.org/10.1016/j.carbpol.2013.12.082.
757 [163] S. Hong, Y. Yuan, K. Zhang, H. Lian, H. Liimatainen, Efficient Hydrolysis of Chitin in a Deep Eutectic
758 Solvent Synergism for Production of Chitin Nanocrystals, Nanomaterials, 2020.
759 [164] Y. Yuan, S. Hong, H. Lian, K. Zhang, H. Liimatainen, Comparison of acidic deep eutectic solvents
760 in production of chitin nanocrystals, Carbohydrate Polymers 236 (2020) 116095.
761 https://doi.org/https://doi.org/10.1016/j.carbpol.2020.116095.
762 [165] Z. Li, C. Liu, S. Hong, H. Lian, C. Mei, J. Lee, Q. Wu, M.A. Hubbe, M.-C. Li, Recent advances in
763 extraction and processing of chitin using deep eutectic solvents, Chemical Engineering Journal 446
764 (2022) 136953. https://doi.org/https://doi.org/10.1016/j.cej.2022.136953.
765 [166] J. Jiang, N.C. Carrillo-Enríquez, H. Oguzlu, X. Han, R. Bi, M. Song, J.N. Saddler, R.-C. Sun, F. Jiang,
766 High Production Yield and More Thermally Stable Lignin-Containing Cellulose Nanocrystals Isolated
767 Using a Ternary Acidic Deep Eutectic Solvent, ACS Sustainable Chemistry & Engineering 8(18) (2020)
768 7182-7191. https://doi.org/10.1021/acssuschemeng.0c01724.

[167] C. Liu, M.-C. Li, W. Chen, R. Huang, S. Hong, Q. Wu, C. Mei, Production of lignin-containing cellulose nanofibers using deep eutectic solvents for UV-absorbing polymer reinforcement, Carbohydrate Polymers 246 (2020) 116548. https://doi.org/https://doi.org/10.1016/j.carbpol.2020.116548.
[168] X. Li, C. Ning, L. Li, W. Liu, Q. Ren, Q. Hou, Fabricating lignin-containing cellulose nanofibrils with unique properties from agricultural residues with assistance of deep eutectic solvents, Carbohydrate Polymers 274 (2021) 118650. https://doi.org/https://doi.org/10.1016/j.carbpol.2021.118650.
[169] Q. Zhang, R. Ma, L. Ma, L. Zhang, Y. Fan, Z. Wang, Contribution of lignin in esterified lignocellulose nanofibers (LCNFs) prepared by deep eutectic solvent treatment to the interface compatibility of LCNF/PLA composites, Industrial Crops and Products 166 (2021) 113460. https://doi.org/https://doi.org/10.1016/j.indcrop.2021.113460.
[170] X. Tan, W. Zhao, T. Mu, Controllable exfoliation of natural silk fibers into nanofibrils by protein denaturant deep eutectic solvent: nanofibrous strategy for multifunctional membranes, Green Chemistry 20(15) (2018) 3625-3633. https://doi.org/10.1039/C8GC01609G.
[171] Y. Wang, Z. Yang, B. Jia, L. Chen, C. Yan, F. Peng, T. Mu, Z. Xue, Natural Deep Eutectic Solvent-Assisted Construction of Silk Nanofibrils/Boron Nitride Nanosheets Membranes with Enhanced Heat-Dissipating Efficiency, Advanced Science n/a(n/a) (2024) 2403724. https://doi.org/https://doi.org/10.1002/advs.202403724.
[172] P. Zamani, J. Ozdemir, Y. Ha, M. Benamara, A.V. Kuchuk, T. Wang, J. Chen, A.R. Khosropour, M.H. Beyzavi, Magnetic Nanoparticle Anchored Deep Eutectic Solvents as a Catalyst for the Etherification and Amination of Naphthols, Advanced Synthesis & Catalysis 360(22) (2018) 4372-4380. https://doi.org/https://doi.org/10.1002/adsc.201800743.
[173] X. Zhao, X. Lan, D. Yu, H. Fu, Z. Liu, T. Mu, Deep eutectic-solvothermal synthesis of nanostructured Fe3S4 for electrochemical N2 fixation under ambient conditions, Chemical Communications 54(92) (2018) 13010-13013. https://doi.org/10.1039/C8CC08045C.
[174] X. Zhao, Z. Xue, W. Chen, Y. Wang, T. Mu, Eutectic Synthesis of High-Entropy Metal Phosphides for Electrocatalytic Water Splitting, ChemSusChem 13(8) (2020) 2038-2042. https://doi.org/https://doi.org/10.1002/cssc.202000173.
[175] H. Mou, J. Wang, D. Zhang, D. Yu, W. Chen, D. Wang, T. Mu, A one-step deep eutectic solvent assisted synthesis of carbon nitride/metal oxide composites for photocatalytic nitrogen fixation, Journal of Materials Chemistry A 7(10) (2019) 5719-5725. https://doi.org/10.1039/C8TA11681D.
[176] X. Zhao, Z. Xue, W. Chen, X. Bai, R. Shi, T. Mu, Ambient fast, large-scale synthesis of entropy-stabilized metal–organic framework nanosheets for electrocatalytic oxygen evolution, Journal of Materials Chemistry A 7(46) (2019) 26238-26242. https://doi.org/10.1039/C9TA09975A.
[177] S. Liu, B. Zhang, Z. Yang, Z. Xue, T. Mu, Deep eutectic solvothermal NiS2/CdS synthesis for the visible-light-driven valorization of the biomass intermediate 5-hydroxymethylfurfural (HMF) integrated with H2 production, Green Chemistry 25(7) (2023) 2620-2628. https://doi.org/10.1039/D2GC04535D.
[178] S.V. Mohite, S. Kim, C. Lee, J. Bae, Y. Kim, Z-scheme heterojunction photocatalyst: Deep eutectic solvents-assisted synthesis of Cu2O nanocluster improved hydrogen production of TiO2, Journal of Alloys and Compounds 928 (2022) 167168. https://doi.org/https://doi.org/10.1016/j.jallcom.2022.167168.
[179] M. Karimi, M.J. Eshraghi, V. Jahangir, A facile and green synthetic approach based on deep eutectic solvents toward synthesis of CZTS nanoparticles, Materials Letters 171 (2016) 100-103. https://doi.org/https://doi.org/10.1016/j.matlet.2016.02.065.
[180] R. Manikandan, S. Sadhasivam, S. Lee, C. Seung-Cheol, K. Ashok Kumar, C. Bathula, V. Gopalan Sree, D. Young Kim, S. Sekar, Deep eutectic solvents assisted synthesis of AC-decorated NiO nanocomposites for hydrogen evolution reaction, Journal of Molecular Liquids 375 (2023) 121338. https://doi.org/https://doi.org/10.1016/j.molliq.2023.121338.

[181] C. Li, O.J.H. Chai, Q. Yao, Z. Liu, L. Wang, H. Wang, J. Xie, Electrocatalysis of gold-based nanoparticles and nanoclusters, Materials Horizons 8(6) (2021) 1657-1682. https://doi.org/10.1039/D0MH01947J.
[182] N. Azizi, M. Edrisi, Z. Manochehri, Greenersynthesisof magnetic nanoparticles in an aqueous deepeutectic solvent, Scientia Iranica 23(6) (2016) 2750-2755.
[183] F. Zhou, D. Shi, W. Mu, S. Wang, Z. Wang, C. Wei, R. Li, T. Mu, Machine learning models accelerate deep eutectic solvent discovery for the recycling of lithium-ion battery cathodes, Green Chemistry 26(13) (2024) 7857-7868. https://doi.org/10.1039/D4GC01418A.
[184] Á. Santana-Mayor, R. Rodríguez-Ramos, B. Socas-Rodríguez, M.d.M. Afonso, J.A. Palenzuela, Combinations of Nanomaterials and Deep Eutectic Solvents as Innovative Materials in Food Analysis, Processes 9(12) (2021) 2131.
[185] W. da Silva, M.E. Ghica, C.M.A. Brett, Novel nanocomposite film modified electrode based on poly(brilliant cresyl blue)-deep eutectic solvent/carbon nanotubes and its biosensing applications, Electrochimica Acta 317 (2019) 766-777. https://doi.org/https://doi.org/10.1016/j.electacta.2019.06.003.
[186] X. Li, K.H. Row, Preparation of deep eutectic solvent-based hexagonal boron nitride-molecularly imprinted polymer nanoparticles for solid phase extraction of flavonoids, Microchimica Acta 186(12) (2019) 753. https://doi.org/10.1007/s00604-019-3885-8.
[187] H. Ul Haq, R. Bibi, M. Balal Arain, F. Safi, S. Ullah, R. Castro-Muñoz, G. Boczkaj, Deep eutectic solvent (DES) with silver nanoparticles (Ag-NPs) based assay for analysis of lead (II) in edible oils, Food Chemistry 379 (2022) 132085. https://doi.org/https://doi.org/10.1016/j.foodchem.2022.132085.
[188] M. O'Neill, V.S. Raghuwanshi, R. Wendt, M. Wollgarten, A. Hoell, K. Rademann, Gold nanoparticles in novel green deep eutectic solvents: Self-limited growth, self-assembly & catalytic implications, Zeitschrift für Physikalische Chemie 229(1-2) (2015) 221-234.
[189] L. Nie, S. Toufouki, S. Yao, D. Guo, Rethinking the applications of ionic liquids and deep eutectic solvents in innovative nano-sorbents, Frontiers in Chemistry 9 (2021) 653238.
[190] L. Xu, J. Yin, Y. Luo, H. Liu, H. Li, L. Zhu, J. He, W. Jiang, W. Zhu, H. Li, Rational Design of Caprolactam-Based Deep Eutectic Solvents for Extractive Desulfurization of Diesel Fuel and Mechanism Study, ACS Sustainable Chemistry & Engineering 10(14) (2022) 4551-4560. https://doi.org/10.1021/acssuschemeng.1c08413.
[191] A. Rubin Pedrazzo, C. Cecone, F. Trotta, M. Zanetti, Mechanosynthesis of β-Cyclodextrin Polymers Based on Natural Deep Eutectic Solvents, ACS Sustainable Chemistry & Engineering 9(44) (2021) 14881-14889. https://doi.org/10.1021/acssuschemeng.1c04988.
[192] S. Jemli, D. Pinto, W.G. Kanhounnon, F. Ben Amara, L. Sellaoui, A. Bonilla-Petriciolet, F. Dhaouadi, R. Ameri, L.F.O. Silva, S. Bejar, G.L. Dotto, M. Badawi, Green β-cyclodextrin nanosponges for the efficient adsorption of light rare earth elements: Cerium and lanthanum, Chemical Engineering Journal 466 (2023) 143108. https://doi.org/https://doi.org/10.1016/j.cej.2023.143108.
[193] T. Luo, C. Wang, X. Ji, G. Yang, J. Chen, S. Janaswamy, G. Lyu, Preparation and Characterization of Size-Controlled Lignin Nanoparticles with Deep Eutectic Solvents by Nanoprecipitation, Molecules 26(1) (2021) 218.
[194] T. Luo, Y. Hao, C. Wang, W. Jiang, X. Ji, G. Yang, J. Chen, S. Janaswamy, G. Lyu, Lignin Nanoparticles and Alginate Gel Beads: Preparation, Characterization and Removal of Methylene Blue, Nanomaterials 12(1) (2022) 176.
[195] M. Khatri, Z. Khatri, S. El-Ghazali, N. Hussain, U.A. Qureshi, S. Kobayashi, F. Ahmed, I.S. Kim, Zein nanofibers via deep eutectic solvent electrospinning: tunable morphology with super hydrophilic properties, Scientific Reports 10(1) (2020) 15307. https://doi.org/10.1038/s41598-020-72337-4.
[196] M.K. AlOmar, M.A. Alsaadi, M. Hayyan, S. Akib, R.K. Ibrahim, M.A. Hashim, Lead removal from water by choline chloride based deep eutectic solvents functionalized carbon nanotubes, Journal of Molecular Liquids 222 (2016) 883-894. https://doi.org/https://doi.org/10.1016/j.molliq.2016.07.074.
[197] T. Luo, C. Wang, X. Ji, G. Yang, J. Chen, C.G. Yoo, S. Janaswamy, G. Lyu, Innovative production of lignin nanoparticles using deep eutectic solvents for multifunctional nanocomposites, International

Journal of Biological Macromolecules 183 (2021) 781-789. https://doi.org/https://doi.org/10.1016/j.ijbiomac.2021.05.005.
[198] Y. Zhou, W. Xu, Y. Pan, F. Wang, X. Hu, Y. Lu, M. Jiang, Deep Eutectic-like Solvents: Promising Green Media for Biomass Treatment and Preparation of Nanomaterials, BioResources 17(3) (2022).
[199] I.A. Lawal, M.M. Lawal, M.A. Azeez, P. Ndungu, Theoretical and experimental adsorption studies of phenol and crystal violet dye on carbon nanotube functionalized with deep eutectic solvent, Journal of Molecular Liquids 288 (2019) 110895. https://doi.org/https://doi.org/10.1016/j.molliq.2019.110895.
[200] Z. Ling, F. Xu, J.V. Edwards, N.T. Prevost, S. Nam, B.D. Condon, A.D. French, Nanocellulose as a colorimetric biosensor for effective and facile detection of human neutrophil elastase, Carbohydrate Polymers 216 (2019) 360-368. https://doi.org/https://doi.org/10.1016/j.carbpol.2019.04.027.
[201] A.M. Abdelkader, I.A. Kinloch, Mechanochemical Exfoliation of 2D Crystals in Deep Eutectic Solvents, ACS Sustainable Chemistry & Engineering 4(8) (2016) 4465-4472. https://doi.org/10.1021/acssuschemeng.6b01195.
[202] S. Tuntarawongsa, T. Phaechamud, Polymeric eutectic system, Advanced Materials Research, Trans Tech Publ, 2012, pp. 180-183.
[203] I.M. Aroso, R. Craveiro, Â. Rocha, M. Dionísio, S. Barreiros, R.L. Reis, A. Paiva, A.R.C. Duarte, Design of controlled release systems for THEDES—Therapeutic deep eutectic solvents, using supercritical fluid technology, International Journal of Pharmaceutics 492(1) (2015) 73-79. https://doi.org/https://doi.org/10.1016/j.ijpharm.2015.06.038.
[204] M.C. Serrano, M.C. Gutiérrez, R. Jiménez, M.L. Ferrer, F.d. Monte, Synthesis of novel lidocaine-releasing poly(diol-co-citrate) elastomers by using deep eutectic solvents, Chemical Communications 48(4) (2012) 579-581. https://doi.org/10.1039/C1CC15284J.
[205] L. Douard, J. Bras, T. Encinas, M.N. Belgacem, Natural acidic deep eutectic solvent to obtain cellulose nanocrystals using the design of experience approach, Carbohydrate Polymers 252 (2021) 117136. https://doi.org/https://doi.org/10.1016/j.carbpol.2020.117136.
[206] O. Długosz, M. Ochnik, M. Sochocka, D. Franz, B. Orzechowska, C.-K. Anna, D. Agata, M. Banach, Antimicrobial and antiviral activity of selenium sulphide nanoparticles synthesised in extracts from spices in natural deep eutectic solvents (NDES), Sustainable Materials and Technologies 32 (2022) e00433. https://doi.org/https://doi.org/10.1016/j.susmat.2022.e00433.
[207] Q. Zaib, M.J. Eckelman, Y. Yang, D. Kyung, Are deep eutectic solvents really green?: A life-cycle perspective, Green Chemistry 24(20) (2022) 7924-7930.
[208] G.M. Martínez, G.G. Townley, R.M. Martínez-Espinosa, Controversy on the toxic nature of Deep eutectic solvents and their potential contribution to environmental pollution, Heliyon (2022) e12567.
[209] Z. Li, J.K. Muiruri, J.C.C. Yeo, K.Y. Tang, K. Li, E. Ye, X.J. Loh, Rapid Dissolution of High Concentration Poly (3-hydroxybutyrate) using Neoteric Biosolvent: Experiment and molecular dynamics simulation, Green Chemistry (2023).
[210] K. Radošević, M. Cvjetko Bubalo, V. Gaurina Srček, D. Grgas, T. Landeka Dragičević, I. Radojčić Redovniković, Evaluation of toxicity and biodegradability of choline chloride based deep eutectic solvents, Ecotoxicology and Environmental Safety 112 (2015) 46-53. https://doi.org/https://doi.org/10.1016/j.ecoenv.2014.09.034.
[211] I. Juneidi, M. Hayyan, M.A. Hashim, Evaluation of toxicity and biodegradability for cholinium-based deep eutectic solvents, RSC advances 5(102) (2015) 83636-83647.
[212] OECD, Test No. 301: Ready Biodegradability, OECD Publishing Paris, 1992.
[213] K. Radošević, J. Železnjak, M.C. Bubalo, I.R. Redovniković, I. Slivac, V.G. Srček, Comparative in vitro study of cholinium-based ionic liquids and deep eutectic solvents toward fish cell line, Ecotoxicology and environmental safety 131 (2016) 30-36.
[214] O.S. Hammond, A.-V. Mudring, Ionic liquids and deep eutectics as a transformative platform for the synthesis of nanomaterials, Chemical Communications 58(24) (2022) 3865-3892.

[215] S. Nejrotti, A. Antenucci, C. Pontremoli, L. Gontrani, N. Barbero, M. Carbone, M. Bonomo, Critical Assessment of the Sustainability of Deep Eutectic Solvents: A Case Study on Six Choline Chloride-Based Mixtures, ACS omega (2022).
[216] Y. Chen, T. Mu, Revisiting greenness of ionic liquids and deep eutectic solvents, Green Chemical Engineering 2(2) (2021) 174-186. https://doi.org/https://doi.org/10.1016/j.gce.2021.01.004.